Limnol. Oceanogr., 49(3), 2004, 821–838

Reach-scale isotope tracer experiment to quantify denitrification and related processes in a nitrate-rich stream, midcontinent United States

John Karl Böhlke,[1] *Judson W. Harvey, and Mary A. Voytek*
U.S. Geological Survey, 431 National Center, Reston, Virginia 20192

Abstract

We conducted an in-stream tracer experiment with Br and ^{15}N-enriched NO_3^- to determine the rates of denitrification and related processes in a gaining NO_3^--rich stream in an agricultural watershed in the upper Mississippi basin in September 2001. We determined reach-averaged rates of N fluxes and reactions from isotopic analyses of NO_3^-, NO_2^-, N_2, and suspended particulate N in conjunction with other data in a 1.2-km reach by using a forward time-stepping numerical simulation that included groundwater discharge, denitrification, nitrification, assimilation, and air–water gas exchange with changing temperature. Denitrification was indicated by a systematic downstream increase in the $\delta^{15}N$ values of dissolved N_2. The reach-averaged rate of denitrification of surface-water NO_3^- indicated by the isotope tracer was approximately 120 ± 20 μmol m^{-2} h^{-1} (corresponding to zero- and first-order rate constants of 0.63 μmol L^{-1} h^{-1} and 0.009 h^{-1}, respectively). The overall rate of NO_3^- loss by processes other than denitrification (between 0 and about 200 μmol m^{-2} h^{-1}) probably was less than the denitrification rate but had a large relative uncertainty because the NO_3^- load was large and was increasing through the reach. The rates of denitrification and other losses would have been sufficient to reduce the stream NO_3^- load substantially in the absence of NO_3^- sources, but the losses were more than offset by nitrification and groundwater NO_3^- inputs at a combined rate of about 500–700 μmol m^{-2} h^{-1}. Despite the importance of denitrification, the overall mass fluxes of N_2 were dominated by discharge of denitrified groundwater and air–water gas exchange in response to changing temperature, whereas the flux of N_2 attributed to denitrification was relatively small. The in-stream isotope tracer experiment provided a sensitive direct reach-scale measurement of denitrification and related processes in a NO_3^--rich stream where other mass-balance methods were not suitable because of insufficient sensitivity or offsetting sources and sinks. Despite the increasing NO_3^- load in the experimental reach, the isotope tracer data indicate that denitrification was a substantial permanent sink for N leaving this agricultural watershed during low-flow conditions.

Nutrient enrichment from anthropogenic sources is one of the major stresses affecting aquatic ecosystems. Large amounts of nitrate (NO_3^-) discharged from agricultural watersheds can enter N-sensitive estuaries and coastal marine waters and contribute to increased primary productivity, excessive deep-water oxygen demand, and hypoxia (e.g., Gulf of Mexico, Goolsby et al. 2001; Rabalais et al. 2001). Increased fluxes of NO_3^- in many streams and rivers can be related to changes in land use and agricultural practices, but these relations are complicated because of N transformations within the drainage networks. Efforts to understand regional fluxes of N and to predict aquatic ecosystem responses to agricultural N management practices are hampered by uncertainties about transport, storage, and loss processes affecting NO_3^- in streams and rivers.

Small-scale field and laboratory studies using a variety of techniques have indicated that NO_3^- in oxygenated surface waters can be reduced by benthic denitrification, in which bacteria reduce NO_3^- to N_2 at or below the sediment–water interface (Seitzinger 1988; Nielsen 1992; Jensen et al. 1994; Cornwell et al. 1999; Herbert 1999; Kemp and Dodds 2002*a*). Large-scale regional models and statistical analyses have indicated that N loads in streams and rivers are reduced substantially by a variety of processes of which benthic denitrification is suspected to be a major component (Howarth et al. 1996; Nixon et al. 1996; Alexander et al. 2000; Seitzinger et al. 2002). Although these observations are qualitatively consistent, the results of local empirical studies are variable, and accurate estimates of nitrogen losses in streams and rivers at the reach scale are especially difficult to obtain. Thus, there is considerable uncertainty about the importance of denitrification in streams, especially those with high NO_3^- concentrations in agricultural watersheds. Denitrification is a particularly important process to quantify because it removes NO_3^- from aquatic systems as a largely nonreactive gas, whereas NO_3^--N affected by other processes such as assimilation, burial, and reduction to NH_4^+ remains within the potentially reactive N reservoir.

At the reach scale, studies of NO_3^- loads in streams may indicate overall net gains or losses but may overlook important in-stream N cycling and inputs from groundwater. In-stream addition of NO_3^- with conservative tracers can pro-

[1] Corresponding author (jkbohlke@usgs.gov).

Acknowledgments

This tracer experiment was part of a larger study of nitrogen transport in the Iroquois basin carried out in collaboration with Richard L. Smith and Ron Antweiler (USGS, Boulder), Lesley Smith (U. of Colorado), and Andrew Laursen (Ryerson U.). Assistance in the field and in the USGS laboratories was provided by Julie Kirshtein, Eric Nemeth, Jessica Newlin, Deborah Repert, Janet Hannon, Stan Mroczkowski, Peggy Widman, and Michael Doughten. Richard L. Smith, Andrew Laursen, and Craig Tobias provided helpful data, discussions, and comments. We also thank Steven Thomas and an anonymous journal reviewer for excellent reviews of the manuscript and P. Mulholland and coauthors for sharing their results. This study was supported by the USDA Cooperative State Research, Education, and Extension Service (National Research Initiative Competitive Grants Program in Watershed Processes and Water Resources) and the USGS National Research Program in Water Resources.

vide more information about NO_3^- transport and removal (Valett et al. 1996; Mulholland et al. 2002; Hall and Tank 2003) but does not give direct evidence of denitrification and may cause changes in processes whose rates depend on the NO_3^- concentration (Mulholland et al. 2002). Recent studies have indicated that reach-scale denitrification rates can be derived simply from precise measurements of Ar and N_2 concentrations in streams, combined with numerical simulations of gas fluxes between the stream benthos and the atmosphere (Laursen and Seitzinger 2002; McCutchan et al. 2003). The accuracy of this technique largely depends on knowledge of air–water gas exchange rates, and it may be relatively insensitive in shallow streams (tens of centimeters or less) with appreciable gas-transfer rates. In addition, excess N_2 may be present in streams as a result of dissolution of air bubbles, discharge of N_2-rich groundwater, or other processes that can alter both N_2 concentrations and N_2 : Ar ratios in the absence of denitrification. Other studies have used ^{15}N-enriched NH_4^+ tracers in small streams and ^{15}N-enriched NO_3^- tracers in estuaries to investigate N cycling at the reach scale (Peterson et al. 2001; Tobias et al. 2003). These approaches have yielded information about several components of the N cycle in surface waters, but they have been conducted mainly in systems with relatively low NO_3^- concentrations (typically <5 μmol L^{-1} in the stream studies), and they have addressed denitrification only indirectly.

Experiments involving isotopic tracers as a direct means to estimate reach-scale denitrification rates began only recently, especially in streams with relatively high NO_3^- loads. Injection of $^{15}NO_3^-$ into streams and measurement of the isotopically labeled N_2 produced by denitrification has the potential to improve the quantification of in-stream denitrification substantially. The purpose of the current study was to evaluate the isotope tracer method using ^{15}N-enriched NO_3^- for determining in-stream denitrification rates and N_2 fluxes in an agricultural watershed. This paper presents results of an experiment that involved continuous injection of Br and ^{15}N-enriched NO_3^- at an upstream site and measurement of Br and the concentrations and isotopic compositions of NO_3^-, NO_2^-, N_2 gas, and suspended particulate N at downstream locations in a 1.2-km reach. Results were simulated numerically to determine rates of denitrification, nitrification, assimilation, and groundwater discharge affecting the flux of NO_3^- through the reach. Sensitivity analyses were done to evaluate some of the major sources of uncertainty and ambiguity in experiments of this type, such as gas-transfer rates, composition of groundwater discharge, and significance of intermediate N species. We also contrast our methods and results with those of a similar independent study in a forested watershed (Mulholland et al. 2004).

Site description

The isotope tracer experiment was conducted in a second-order incised reach of Sugar Creek in Benton County, northwestern Indiana (Fig. 1). Sugar Creek is a tributary of the Iroquois, Illinois, and Mississippi river systems. Land use in the Sugar Creek watershed is between 95% and 100% agriculture, predominantly corn and soybeans. Many of the

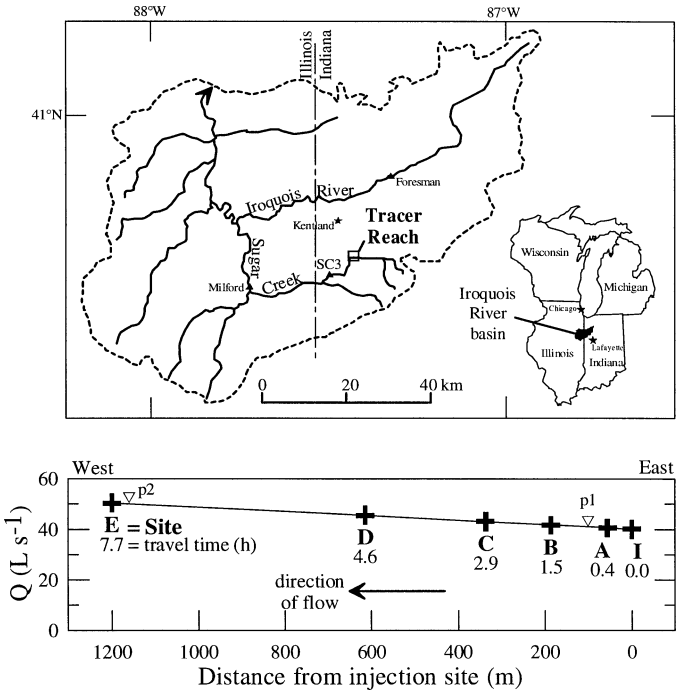

Fig. 1. Location map and schematic diagram of the tracer reach showing the injection site (I), five sampling sites (A to E), and two drainpipes (p1, p2). Travel times and stream-flow values were calculated from Br tracer data (Table 1; Fig. 4).

fields are drained by underground pipes that discharge from the walls of the incised stream channel when water levels are relatively high (mainly winter and spring) but commonly cease flowing when water levels are low (late summer and early fall). Concentrations of NO_3^- in the stream are positively correlated with stream flow and range from <100 μmol L^{-1} in late summer to $>1{,}000$ μmol L^{-1} in winter and spring (Antweiler et al. unpubl. data). Flow measurements indicate that the tracer reach is within an area where Sugar Creek typically gains flow as a result of groundwater discharge. Other evidence for groundwater discharge comes from water-level measurements in piezometers with 0.1-m screens located 0.3 to 1.5 m below the streambed. Water levels in these piezometers ranged from about 0 to 7 cm above the surface of the stream and indicate discharge hydraulic-head gradients from about 0 to 0.07.

Sugar Creek was modified by channelization in the past, as were many of the streams in this agricultural area. The incised valley containing the tracer reach was about 5–10 m wide and was bounded by steep banks from about 2–4 m high. Within the banks, the stream exhibited substantial variation in geomorphology, with pools, riffles, meanders, and islands having formed by sediment remobilization. Streambottom sediments ranged from gravel to fine sand and silt, with scattered aquatic and emergent plant communities. Sediment organic carbon concentrations ranged from about 0.1% to 6%. Laboratory incubation experiments with intact sediment cores indicate that local benthic denitrification rates in Sugar Creek vary by more than an order of magnitude as a result of small-scale variations in sediment characteristics

and biota (M. A. Voytek et al. unpubl. data; L. K. Smith et al. unpubl. data).

The isotope tracer experiment was conducted in September 2001 at a time of relatively low flow (40–50 L s^{-1}) and low NO_3^- concentration (60–70 μmol L^{-1}). These conditions permitted inexpensive enrichment of the ^{15}N of the NO_3^- for approximately 7 h, which was long enough to yield steady-state values in the major solute reservoirs within the reach. The tracer reach was approximately 1200 m long, with five collection sites located at increasing distances downstream from the injection site: A = 55 m, B = 186 m, C = 336 m, D = 615 m, E = 1,200 m (Fig. 1). Measurements at 17 cross-sections between sites A and D yielded a mean depth of 0.19 ± 0.09 m and a mean active channel width of 4.5 ± 2.4 m. The total travel time through the reach was approximately 8 h, which was judged to be sufficient because it bracketed the residence times of previous core incubation experiments that yielded measurable benthic denitrification rates.

Methods

Tracer injection—The tracer injection was designed to give high plateau concentrations of Br and $^{15}NO_3^-$ in the stream with relatively little alteration of the total NO_3^- concentration. The tracer injection solution (injectate) consisted of 32.6 liters of distilled water, 545 g KNO_3 (~17% ^{15}N), 25 g $NaNO_3$ (98% ^{15}N), and 7,030 g KBr, yielding a solution with 1.812 mol L^{-1} of Br and about 0.174 mol L^{-1} of NO_3^- with a composite ^{15}N mole fraction ($X(^{15}N) = n(^{15}N)/[n(^{15}N) + n(^{14}N)]$) of about 0.215. The injectate was dripped into a turbulent riffle using a metering pump at a constant rate of 1.27 ± 0.02 ml s^{-1}, yielding a tracer-dilution factor (injection rate : stream flow) of approximately 3×10^{-5}. The injection lasted for 7.1 h, from 1345 h to 2050 h, and resulted in a period of steady-state (plateau) concentrations of Br (maximum of 59 μmol L^{-1}) and $X(^{15}N)$ of NO_3^- (maximum of 0.020) for at least 2–3 h at each of the downstream collection sites except E. The tracer injection resulted in a slight increase in the stream NO_3^- concentration of about 8%, as indicated by the isotope mass balance near the injection site. This change is within the range of natural variation observed in the stream during base-flow over a period of 1–2 d.

Water sampling and chemical analyses—Stream samples were collected for analyses of Br, NO_3^-, NO_2^-, N_2O, N_2, and suspended particulate N (PN) concentrations and for N-isotopic analyses of NO_3^-, NO_2^-, N_2, and PN. Sampling schedules were guided by results of a preliminary pulse-injection of rhodamine the day before the tracer experiment. Samples for Br tracer breakthrough analysis were collected manually and with an automated water sampler (ISCO, Inc.) at sites A, B, and C at time intervals ranging from 0.5 to 15 min. Samples for Br and $^{15}NO_3^-$ tracer breakthrough analysis were collected with an ISCO autosampler at site D (15-min intervals for 6 h), and site E (30-min intervals for 11.5 h). These samples were kept on ice overnight and filtered the following day. Additional samples for multicomponent analyses of major ions, dissolved gases, and N isotopes during the tracer plateau were collected at approximately 1–2 h intervals during the passage of the plateau at all five sites (four to six samples per site). Two background samples were collected 5 m upstream from the injection site with dedicated nontracer equipment. In addition, because of the potential importance of groundwater discharge, samples of groundwater beneath the stream were collected during several visits to the site by using a peristaltic pump attached to 9-mm outer diameter (OD) stainless steel piezometers with 5-cm screens at depths between 0.3 and 1.5 m beneath the sediment–water interface.

Samples for anion analyses were filtered (0.2 μm) and either frozen or preserved with KOH (pH > 11). Br and NO_3^- concentrations were measured with a Dionex ion chromatograph. NO_2^- concentrations were measured with an ALPKEM auto-analyzer at the U.S. Geological Survey (USGS) laboratory in Boulder, Colorado (R. L. Smith pers. comm. 2002). Stream samples to be analyzed for major dissolved gases (Ar, N_2, O_2, CH_4) were collected in 160-ml capacity serum bottles, unfiltered, without headspace, with KOH as preservative. In the field, each bottle was filled gently from the bottom up, two pellets of reagent KOH (approximately 200 mg total) were dropped in, and a thick butyl rubber stopper (Bellco) was inserted into the bottle with a syringe needle in place to permit excess water to escape. In the laboratory, approximately 10 ml of water was extracted through a syringe needle with a vacuum pump, leaving low-pressure headspace that was equilibrated with the remaining water. Gas analyses of the low-pressure headspace were done in the USGS dissolved-gas laboratory in Reston, Virginia, with a modified Hewlett-Packard 5890 gas chromatograph (GC) with dual separation columns (http://water.usgs.gov/lab/dissolved-gas). Total aqueous gas concentrations were calculated from the headspace concentrations and confirmed by analyses of water equilibrated with laboratory air, with typical uncertainties of around ±0.5–1.0% for Ar and N_2. Analyses done over a period from about 1–6 months after collection indicate that the dissolved-gas concentrations were stable during storage to within the stated uncertainties.

Isotopic analyses of nitrate, nitrite, and suspended particulate nitrogen—The N-isotopic compositions of NO_3^- and NO_2^- were measured together to assess the total N reservoir subject to denitrification. In addition, the isotopic composition of NO_2^- was analyzed separately to determine the role of NO_2^- as an intermediate species in the transfer of tracer ^{15}N from NO_3^- to N_2. These samples were filtered in the field (0.2 μm), preserved with KOH (pH > 11), and stored frozen. Three types of sample aliquots were prepared for mass spectrometry: combined $NO_3^- + NO_2^-$ in whole filtered water, combined $NO_3^- + NO_2^-$ separated from water by solid-phase extraction on a short column (short SPE), and NO_2^- separated by solid-phase extraction on a long column (long SPE). In the short SPE method, sample aliquots containing approximately 20 μmol of NO_3^- were pumped through a 1-cm diameter glass column packed with 5 ml of AG1-X8 anion exchange resin (100–200 mesh) in the Cl form, then eluted slowly with 0.5 N KCl into a series of 5-ml vials. The concentration of $NO_3^- + NO_2^-$ in each eluent vial was determined qualitatively by a colorimetric drop test (modi-

fied from ASTM Method 418C and USGS Method I-2545-78), and the fraction of the eluent containing all the NO_3^- plus NO_2^- was freeze dried. The selective elution procedure was aimed at minimizing the amounts of Cl^- and other anions (including organic compounds) in the sample. In the long SPE method, sample aliquots containing about 20–40 μmol of NO_3^- and 1–2 μmol of NO_2^- were pumped through a 1-cm diameter glass column packed with 15 ml of AG1-X8 resin in the Cl form then eluted slowly with 0.5 N KCl. Concentrations of NO_2^- and NO_3^- were monitored in the eluent by drop colorimetry, and the fractions containing each species were collected separately and freeze dried.

The N-isotopic analyses were done by two different mass spectrometric (MS) techniques referred to as bacterial MS and off-line MS. For bacterial MS, aliquots containing approximately 10–20 nmol of NO_3^- and(or) NO_2^- were incubated with the denitrifier *Pseudomonas chlororaphis* to produce N_2O, which was purged with He, trapped with liquid N_2, and released in a He carrier stream for analysis by continuous-flow mass spectrometry at $m:z$ 44, 45, and 46 (modified from Sigman et al. 2001). Bacterial MS was used for analysis of combined $NO_3^- + NO_2^-$ in whole filtered water samples and for analysis of NO_2^- separated from samples by long SPE. For off-line MS, aliquots containing 1–5 μmol of NO_3^- and(or) NO_2^- were baked in sealed glass tubes with Cu + Cu_2O and CaO to produce N_2 (modified from Kendall and Grim 1990; Böhlke et al. 1993), which was analyzed by dual-inlet mass spectrometry at $m:z$ 28 and 29 (plus $m:z$ 30 for the injectate). Off-line MS was used for analysis of combined $NO_3^- + NO_2^-$ separated from samples by short SPE. The isotope data are reported as $\delta^{15}N$ values with respect to air N_2 ($\delta^{15}N = [R_i/R_{air} - 1] \times 1{,}000‰$, where R is the isotope mole ratio $n(^{15}N)/n(^{14}N)$ and $R_{air} = 272^{-1}$; Coplen et al. 1992). The mass spectrometry was calibrated by analyses of NO_3^- with known isotopic composition and normalized to $\delta^{15}N$ values of +4,730‰ and +0.4‰ for the international N-isotopic reference materials IAEA-311 and IAEA-N1, respectively (Parr and Clements 1991; Böhlke and Coplen 1995). The relation between $\delta^{15}N$ values (used for describing analytical results) and ^{15}N mole fractions (used in mass-balance calculations) is given by $\delta^{15}N = \{272 \times X(^{15}N)/[1 - X(^{15}N)] - 1\} \times 1{,}000‰$.

Sample treatments were evaluated by analyzing artificial solutions prepared from NO_3^- and NO_2^- with known $\delta^{15}N$ values ranging from +4‰ to +5,625‰ at concentrations similar to those of the stream samples. Results of these tests indicate small biases in the analyses of small samples (NO_2^-) and samples with high $\delta^{15}N$ values (NO_3^-) caused by various procedural N blanks. Blank corrections were made by applying scale factors based on analyses of reference materials as samples (Gonfiantini 1978; Böhlke and Coplen 1995). Scale-factor adjustments indicated blanks typically ranged from about 5% to 9% of the sample N for the off-line N_2 method (mainly from the KCl eluent used for SPE) and 2% to 7% of the sample N for the bacterial N_2O method. After scale adjustments, bacterial MS results were an average of 1.02 ± 0.03 times higher than off-line results for $\delta^{15}N[NO_3^- + NO_2^-]$, which indicates overall uncertainties of the order of ±100‰ to 200‰ for $\delta^{15}N$ values between 3,000‰ and 5,000‰, although the individual methods commonly had better reproducibilities. The reported values of $\delta^{15}N[NO_3^- + NO_2^-]$ are the averages from the two methods and are referred to subsequently as $\delta^{15}N[NO_3^-]$ for convenience. For $\delta^{15}N[NO_2^-]$, the bacterial MS results have estimated uncertainties of the order of ±2‰ to ±20‰ over a range of $\delta^{15}N$ values from 0‰ to 350‰.

Suspended particulate matter was analyzed as a potential biologic sink for tracer ^{15}N from NO_3^- assimilation. Suspended particulate samples for N-isotope analysis were captured during the tracer plateau on precombusted glass-fiber filters (Whatman GF/F), rinsed in the field with deionized water (DIW), and frozen. In the laboratory, the filters were thawed, rinsed again with DIW, then analyzed by the off-line MS technique, with estimated uncertainties of ±0.2–0.3‰.

Isotopic analysis of nitrogen gas—Changes in the N-isotopic composition of aqueous N_2 caused by denitrification of tracer NO_3^- are expected to be small because of the large reservoir of dissolved atmospheric N_2. For precise isotopic analysis of N_2 in stream water, the low-pressure headspace remaining in each 160-ml serum bottle after GC gas analysis was expanded in a high-vacuum extraction line into a pair of 20-cm quartz glass tubes containing Cu_2O + Cu and CaO. The tubes were sealed, baked, and analyzed by dual-inlet mass spectrometry at $m:z$ 28 and 29, as in the off-line MS analyses of $NO_3^- + NO_2^-$. In contrast to some other tracer studies involving ''isotope pairing'' (Nielsen 1992), the ^{15}N enrichment of the NO_3^- tracer in our experiment was low enough that $^{15}N^{15}N$ ($m:z$ 30) was not a significant component of the N_2 formed by denitrification. The dissolved N_2 results were calibrated by analyzing aliquots of air N_2 ($\delta^{15}N = 0‰$) and compared to results from laboratory-equilibrated air-saturated water samples that were collected, prepared, and analyzed the same way as the stream samples. The average $\delta^{15}N[N_2]$ value of lab-equilibrated water samples analyzed with the stream samples was +0.67‰ (±0.07‰, $n = 8$), similar to other published experimental results (Knox et al. 1992). Overall uncertainties of the $\delta^{15}N[N_2]$ values of stream samples are estimated to be approximately ±0.1–0.2‰. Analyses of replicate samples containing $^{15}NO_3^-$ tracer indicate that $\delta^{15}N[N_2]$ values were not altered measurably by diffusion or reactions during storage on time scales of months to years (this study and other unpublished data).

Numerical simulations—To determine reaction rates from the tracer data, information is needed about transport of water and conservative solutes through the tracer reach. In addition, it is important to know whether the major transport reservoirs involved in the reactions were likely to adjust completely to the presence of the tracer on the time scale of the injection. Therefore, the patterns of arrival and breakthrough of tracer Br at four sites (B, C, D, and E) were simulated with the USGS code OTIS-P (one-dimensional transport with inflow and storage with parameter estimation; Runkel 1998). Site A was not included in this analysis because of uncertainty about the tracer arrival time. As input to OTIS-P, streamflow and groundwater inflow were calculated from the injection rate and Br concentration of the tracer injectate and the plateau Br concentrations at each

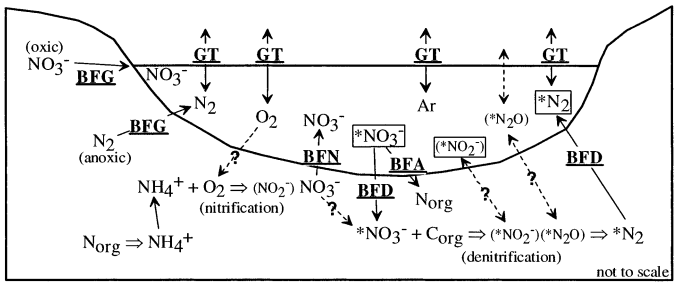

Fig. 2. Conceptual model of selected components of the nitrogen isotope tracer experiment. Underlined acronyms indicate fluxes considered in the numerical simulations (Eqs. 1–6): GT = gas transfer; BFN = benthic flux from nitrification; BFD = benthic flux from denitrification; BFA = benthic flux from assimilation (could include other unspecified NO_3^- losses); BFG = benthic flux from groundwater discharge (may contain either NO_3^- or excess N_2). Asterisks indicate species that acquire tracer ^{15}N. Boxes indicate species analyzed for $\delta^{15}N$.

stream site (Harvey and Wagner 2000). For each subreach, the OTIS-P simulations provided the average tracer velocity, longitudinal dispersion coefficient, cross-sectional areas of the active stream channel and nonchannel transient storage zones, exchange rate between channel and storage zones, water residence time in storage zones, and total travel time for water that includes time spent in storage (Harvey and Wagner 2000).

The rates of denitrification and related processes were determined by constructing a numerical spreadsheet reaction model to simulate changes in the concentrations of Br, Ar, N_2, and NO_3^- and changes in the $\delta^{15}N$ values of N_2 and NO_3^- within a hypothetical parcel of stream water as it moved through the tracer reach. This reaction model includes solute travel times from OTIS-P, variable air–water gas exchange affected by temperature and other gas fluxes, and reach-averaged rates of groundwater discharge, denitrification, nitrification, and NO_3^- assimilation (Fig. 2). Because of the way the model parameters are specified, the ''assimilation'' term could include other unspecified reactive losses of NO_3^-. The simulation was designed to follow a parcel of water that passed the injection site near the end of the injection period at 1830 h. This parcel then passed each of the other sites near the end of the tracer plateau, when the $\delta^{15}N$ values of the intermediate N species and transport reservoirs are considered most likely to have reached a steady state (*see below*). Net O_2 fluxes were included in the simulations because they reflect redox processes that may have affected N reactions.

In the reaction model, fluxes and concentrations of H_2O, Br, and NO_3^- were calculated at each time step from:

$$Q_t = Q_{t-\Delta t} + \Delta Q_{bf} + \Delta Q_{ps} \quad (1)$$

$$C_t = (C_{t-\Delta t} + \Delta C_{bf} + \Delta C_{ps}) \times Q_{t-\Delta t}/Q_t \quad \text{and} \quad (2)$$

$$\Delta C_{bf} = \Delta t/Z \times (\text{BFD} + \text{BFA} + \text{BFN} + \text{BFG}) \times 10^{-3} \quad (3)$$

where Q is streamflow in L s^{-1}, C is aqueous concentration in μmol L^{-1}, t is time in h, Δt is one time step (0.05–0.10 h), Z is mean stream depth in m, and the subscripts bf and ps refer to benthic flux and point source, respectively. Point sources include the tracer injectate and two minor drain pipes (Fig. 1). The benthic fluxes (BF, in μmol m^{-2} h^{-1}) include transfer of NO_3^- from the stream to support denitrification (BFD) or assimilation (BFA), transfer of NO_3^- to the stream from nitrification (BFN), and transfer of water and NO_3^- to the stream from groundwater discharge (BFG). Fluxes are given positive values when species enter the water column and negative values when species leave the water column. All reaction rates are treated as benthic fluxes to facilitate comparison, although they are not all known to be limited to the benthos.

Fluxes and concentrations of Ar, N_2, and O_2 were calculated from:

$$C_t = (C_{t-\Delta t} + \Delta C_{bf} + \Delta C_{ps} + \Delta C_{af}) \times Q_{t-\Delta t}/Q_t \quad (4)$$

$$\Delta C_{bf} = \Delta t/Z \times (\text{BFD} + \text{BFG} + \text{BFO}) \times 10^{-3} \quad \text{and} \quad (5)$$

$$\Delta C_{af} = \Delta t/Z \times \text{GTV}_t \times [C_{eq,t} - (C_{t-\Delta t} + \Delta C_{bf})] \quad (6)$$

where GTV is the gas-transfer velocity in m h^{-1}, BFO is the net benthic reaction flux of O_2, and the subscripts af and eq refer to atmospheric flux and equilibrium, respectively. Equilibrium concentrations of Ar, N_2, and O_2 (Weiss 1970) were calculated from stream temperature at each time step, assuming an elevation of 200 m and 100% relative humidity. Sources of error in the simulation of gas concentrations include deviations from the assumed conditions of atmospheric pressure, humidity, and temperature in the boundary layer, entrainment of excess air, and uncertainties in GTV.

GTV is equivalent to the aqueous diffusion coefficient divided by the thickness of the aqueous film possessing the diffusion gradient (flux divided by concentration), assuming the air is well mixed above the air–water interface and the stream is well mixed below the aqueous diffusion layer. Values of GTV can be calculated from gas-exchange experiments, and they can be estimated from empirical relations with the velocity, depth, and slope of the stream (Bennett and Rathbun 1972) as well as with wind speed (Wanninkhof et al. 1985; Donelan and Wanninkhof 2002). In the current study, values of GTV determined by three different methods were compared: (1) a local correlation between wind speed and GTV_{600} (the gas-transfer velocity of CO_2, with Schmidt number 600), derived from a series of dual-gas injection experiments in Sugar Creek between 1999 and 2001 (Laursen unpubl. data); (2) trial and error simulations to match the rate of change in Ar concentrations during the tracer experiment; (3) a global empirical relation between GTV_{O_2}, stream velocity, and depth (Bennett and Rathbun 1972). Values of GTV for Ar, N_2, and O_2 were estimated from the ratios $\text{GTV}_{Ar}:\text{GTV}_{600} = 1.02$, $\text{GTV}_{N_2}:\text{GTV}_{600} = 0.97$, and $\text{GTV}_{O_2}:\text{GTV}_{600} = 1.01$, derived from the respective Schmidt numbers at the average stream temperature of 18°C.

Isotope effects including transport and reaction of the ^{15}N tracer were incorporated in the simulations by applying Eqs. 1–6 independently to the ^{15}N and ^{14}N components of the NO_3^- and N_2. Molar $^{15}N:^{14}N$ ratios ($R[i]$) and $^{15}N:^{14}N$ fractionation factors ($\alpha[i/j] = R[i]/R[j]$) were assigned to the major N species and reactions: $R[N_{2,air}] = 0.0036765$ ($\delta^{15}N[N_{2,air}] = 0‰$), $\alpha[N_{2,aq}/N_{2,air}]_{equilibrium} = 1.0007$, $\alpha[N_2$ gas transfer$]_{kinetic} = 0.9987$, $\alpha[N_2/NO_3^-]_{denit} = 0.980$, $\alpha[N_{organic}/$

$NO_3^-]_{nitrif}$ = 1.000 (assuming mineralization or NH_4^+ transport is the rate-limiting step), and $R[NO_3^-]_{nitrif}$ = 0.003706 ($\delta^{15}N[NO_3^-]_{nitrif}$ = +8‰; *see below*; Junk and Svec 1958; Hübner 1986; Knox et al. 1992; Montoya 1994). Isotope fractionations generally did not have measurable effects on the overall results of the current tracer simulations, but they were included in the model because of their potential importance in other situations. At each site, the $\delta^{15}N$ value of the NO_3^- undergoing benthic denitrification was assumed to be the same as the $\delta^{15}N$ value of the overlying surface-water NO_3^- by the end of the tracer plateau. Some models also included an intermediate reservoir of NO_2^- that was assumed to have a steady-state concentration but was allowed to evolve isotopically in response to ^{15}N tracer denitrification.

The variables in the reaction model were adjusted in a progressive sequence by trial and error to solve different parts of the problem: (1) water balance—given travel times derived from the OTIS-P transport model along with point-source inputs (Q_{ps}), adjust initial streamflow ($Q°$) and the average rate of groundwater discharge (Q_{bf}) in the reaction model to give a match for the plateau Br concentrations at collection sites A to E; (2) gas transport properties—given average stream velocity and depth (Z) and records of temperature and wind speed, adjust Ar°, $N_2°$, and GTV_{600} (according to the different estimation procedures) until the model gives a reasonable match to the rate of change of Ar and N_2 concentrations over time; (3) nitrate fluxes—given the initial NO_3^- concentration $[NO_3^-]°$, adjust the NO_3^- fluxes caused by groundwater discharge (BFG), nitrification (BFN), and total NO_3^- loss by denitrification plus assimilation (BFD + BFA) until the model results match the observed downstream changes in the values of NO_3^- concentration and $\delta^{15}N[NO_3^-]$; (4) denitrification—adjust denitrification (BFD) until the model results match the observed downstream changes in $\delta^{15}N[NO_3^-]$ and $\delta^{15}N[N_2]$. Because step (3) of this sequence is underdetermined, various assumptions were made about the composition of groundwater discharge to provide limits on BFG and BFN. The denitrification rate derived in step (4) is largely independent of the various NO_3^- flux values derived in step (3). Net reduction of O_2 was treated similarly to the N_2 fluxes.

Results

Results of physical, chemical, and isotopic measurements were used to evaluate transport and reaction processes in the stream and to select targets for the transport and reaction simulations. Constant values of reach-scale process rates were determined such that the data from all of the collection sites were reproduced approximately in a single reaction simulation. The reaction model then was used to test the sensitivity of derived rates to some of the uncertainties in the data and the field situation.

Physical parameters—Temperature and wind are important factors affecting the direction and rate of exchange of gases (including ^{15}N-labeled N_2) across the air–water interface. Wind speed was not measured at the tracer site, but records at Lafayette, Indiana (approximately 40 km southeast of the tracer reach), indicate wind velocities generally decreased from around 6 m s^{-1} near the beginning of the tracer injection to 2 m s^{-1} near the end of the sampling time (Fig. 3). Water temperatures in the tracer reach decreased monotonically from about 21°C to 16°C during the tracer experiment (Fig. 3). Water temperatures in the 24 h preceding the tracer injection were estimated from measurements at site SC3 (approximately 8 km downstream from the tracer reach) and varied between 14°C and 21°C (Fig. 3).

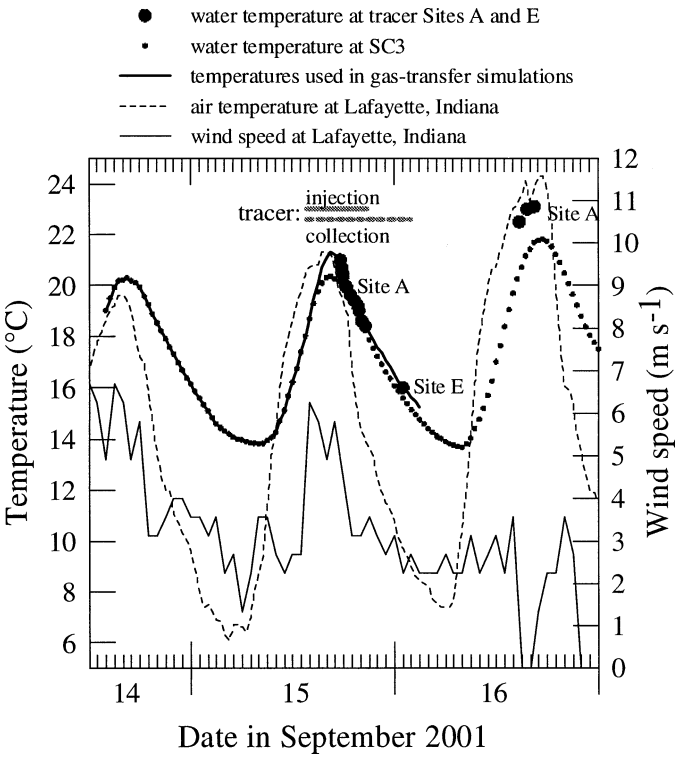

Fig. 3. Measured and estimated water temperatures in Sugar Creek along with measured air temperatures and wind speeds at Lafayette, Indiana (http://shadow.agry.purdue.edu). Data from Sugar Creek site SC3 (approximately 8 km downstream from tracer site E) are from R.L. Smith (unpubl. data). The periods of time corresponding to the tracer injection and sample collection are indicated.

At the beginning of the injection, the tracer reach was under clear sunny sky. Sunset occurred at 1900 h and darkness fell by about 1945 h, approximately 1 h before the end of the injection period. Therefore, early parts of the tracer plateau began in light conditions and ended in the dark, whereas late parts of the tracer plateau passed through the tracer reach mainly in the dark.

Br concentrations and stream transport properties—The Br data were used to quantify stream flow, tracer travel times, interactions with storage zones, and groundwater inputs that might have affected the concentrations and isotopic compositions of NO_3^- and N_2. During the passage of the tracer, Br concentrations at sites A–D achieved a plateau (steady state) condition for 2–4 h. At site E, Br concentrations approached but did not sustain a plateau value before beginning to decrease. Plateau Br concentrations decreased systematically through the reach and indicate a 25% increase in stream flow from 40.0 to 50.2 L s^{-1} (Fig. 4; Table 1). After

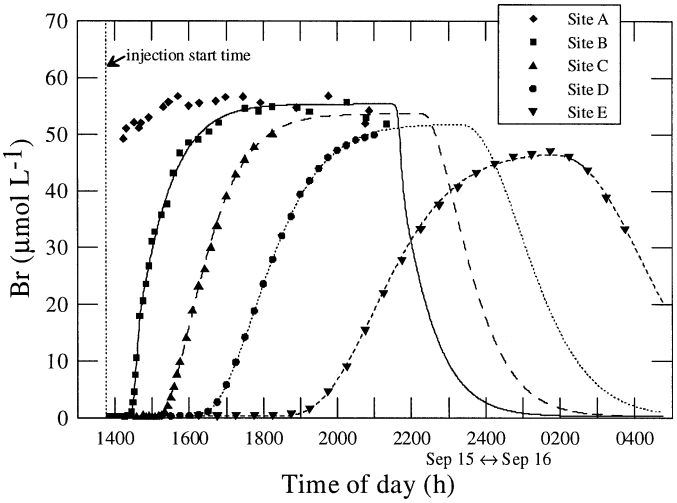

Fig. 4. Breakthrough curves for Br at five sampling sites. Symbols indicate measured values. Curves were calculated by using program OTIS-P (Runkel 1998) with the transport parameters listed in Table 1.

adjustment for minor discharges from two drainage pipes (0.8 L s^{-1} between sites A and B; 0.2 L s^{-1} between sites D and E), the plateau Br data indicate average groundwater contribution to flow of about 0.03 h^{-1} (vertical discharge rates of about 0.005–0.006 m h^{-1}).

Simulations of Br transport with OTIS-P using parameters listed in Table 1 yielded reasonably good fits to the Br breakthrough curves at all five sites (Fig. 4). The total travel times through the subreaches estimated with the OTIS-P model include the time spent in short-term storage reservoirs such as relatively stagnant areas of surface water or the hyporheic zone. Substantial exchange of water and solute between active channel and transient storage zones was indicated by the results (Table 1). Nevertheless, the average time a parcel of water was retained in a storage zone (0.2 to 0.5 h) was short compared to the length of the tracer injection (7 h), which indicates that the tracer achieved steady-state values in the major storage zones by the middle or end of the surface-water plateaus at sites A–D, but perhaps not completely at site E. If the major storage zones include the main reaction sites, then this result supports the use of steady-state reaction parameters to simulate stream data near the end of the tracer plateau.

Nitrate concentrations, fluxes, and isotopes in the stream—Major losses and additions of stream NO_3^- can be resolved by combining the chemical and isotopic mass balances through the reach. The concentration of NO_3^- within the tracer plateau did not change systematically downstream (the average value for all five sites was 71 ± 3 μmol L^{-1}; Table 2). Given the 25% increase in stream flow, this means that the NO_3^- load also increased by about 25% between sites A and E. A simple chemical mass balance for NO_3^- clearly would not detect denitrification in this gaining reach.

Despite the increase in the NO_3^- load, there was a systematic decrease in the flux of tracer ^{15}N going downstream. The plateau flux of tracer $^{15}NO_3^-$ (in μmol s^{-1}) at each site can be derived from the stream flow (Table 1) and the apparent ^{15}N excess over the background ^{15}N in the NO_3^-:

$$\text{Tracer } {}^{15}NO_3^- \text{ flux} = Q \times C[NO_3^-] \times \{X({}^{15}N)[NO_3^-]_{\text{plateau}} - X({}^{15}N)[NO_3^-]_{\text{background}}\} \quad (7)$$

where Q = stream flow in L s^{-1}, $C[NO_3^-]$ is the plateau concentration of NO_3^- in μmol L^{-1}, $X(^{15}N)[NO_3^-]_{\text{plateau}}$ is the mole fraction of ^{15}N in NO_3^- during the tracer plateau, and $X(^{15}N)[NO_3^-]_{\text{background}}$ is the background mole fraction (Table 2; Fig. 5). The tracer $^{15}NO_3^-$ fluxes decreased between sites A and E by about 5.7 μmol s^{-1} (from 46.3 to 40.6 μmol s^{-1}) and can be fit to first-order expressions of total NO_3^- loss (by a combination of denitrification, assimilation, and other processes) with rate constants of around 1.0 (±0.4) × 10^{-4} m^{-1} or 0.017 ± 0.006 h^{-1}. Applying the latter value instantaneously to the average NO_3^- concentration in the tracer plateau (71 μmol L^{-1}) would yield a zero-order total NO_3^- loss rate of around 1.2 μmol L^{-1} h^{-1}.

The tracer breakthrough curves for Br and $X(^{15}N)[NO_3^-]$ indicate two different types of mixing between normal nontracer NO_3^- and tracer NO_3^- in the stream (Fig. 5): (1) Br and $^{15}NO_3^-$ data from the early parts of the breakthrough curves (leading edge of the tracer plateau) indicate relatively conservative mixing between tracer and nontracer stream water resulting from longitudinal dispersion of the tracer cloud in the stream channel and (2) a downstream trend of decreasing plateau values of $X(^{15}N)[NO_3^-]$ indicates addition of nontracer NO_3^- within the reach. The source of the added nontracer NO_3^- could be either nitrification or inflow of NO_3^--bearing groundwater. The combined NO_3^- contribution from these sources was greater than the sum of the NO_3^- losses, but the

Table 1. Transport parameters determined from bromide tracer data and OTIS-P simulation.

Sub-reach	Sub-reach length (m)	Tracer travel time (h)	Stream flow* Q (L s^{-1})	Groundwater input (m^2 s^{-1} ×10^{-6})	Stream dispersion D (m^2 s^{-1})	Stream area A (m^2)	Storage area A_S (m^2)	Storage exchange coefficient α (h^{-1})	Storage residence time† τ_s (h)
I→B	186	1.45	40.0→41.6	8.7	0.05	0.65	0.50	1.66	0.47
B→C	151	1.40	41.6→42.9	8.8	0.03	0.80	0.62	3.53	0.22
C→D	278	1.72	42.9→45.4	8.7	0.04	0.57	0.41	2.02	0.37
D→E	585	3.13	45.4→50.2	7.9	0.04	0.58	0.29	1.44	0.35

* Stream flows are given for the upstream and downstream end of each sub-reach indicated in the left-hand column.
† Storage residence time (τ_s) is equal to $A_s\, A^{-1} \alpha^{-1}$.

Table 2. Tracer plateau values used as targets for the reaction model.

Site	I	A	B	C	D	E
Input values						
Time (h)*	1830	[1856]†	1957	2121	2304	0212
T (°C)‡	19.9	19.6	18.8	17.9	17.0	15.6
Output values						
Br (μmol L^{-1})§	0.2	[58.7]‖	56.4	54.2	51.1	46.7
NO_3^- (μmol L^{-1})§	64	69	72	71	69	73
$\delta^{15}N[NO_3^-]$ (‰)§¶	14	4630	4170	3870	3670	3080
$\delta^{15}N[NO_2^-]$ (‰)	—	30	—	—	300	350
$\delta^{15}N[N_2]$ (‰)#	0.7	1.3	3.2	5.1	7.0	8.6

* Time of day for arrival of a parcel near the end of the tracer plateau.
† Travel time to site A was interpolated between sites I and B by distance.
‡ Smoothed temperature value of the stream at the specified time (*see Fig. 3*).
§ Upstream nontracer values at site I; the average of 3–4 plateau values at sites A to D; the highest value at site E (*see Figs. 8a–e*).
‖ Br concentrations at site A were slightly higher in plateau isotope samples than in tracer breakthrough samples (possibly from incomplete tracer mixing between sites I and A?).
¶ $\delta^{15}N[NO_3^- + NO_2^-]$, average of measurements by off-line MS and bacterial MS.
# Interpolated value for the late plateau parcel (*see Fig. 8f*).

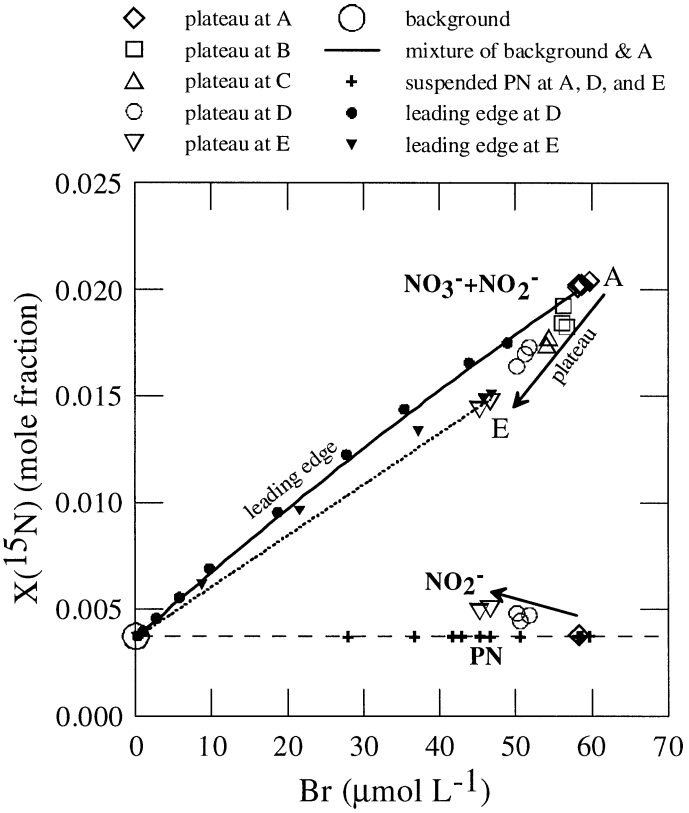

Fig. 5. Relation between Br and ^{15}N mole fractions in NO_3^-, NO_2^-, and suspended PN in stream samples from the tracer plateau and leading edge. For NO_3^-, the solid curve indicates a hypothetical array of conservative mixtures of tracer plateau water at site A with normal (''background'') stream water in the absence of other NO_3^- sources and sinks. Decreasing plateau values from site A to site E indicate dilution of Br and addition of new NO_3^- with nontracer $\delta^{15}N$ from nitrification and(or) groundwater discharge.

relative importance of the two sources cannot be derived from the data in Fig. 5. The positions of the plateau samples below the conservative mixing curve in Fig. 5 could indicate either that the concentration of NO_3^- in discharging groundwater was higher than the plateau stream NO_3^- concentration (>71 μmol L^{-1}) or that a substantial amount of nontracer NO_3^- was from nitrification that was not associated with Br dilution. Both of these possibilities were considered in the reaction simulations (*see below*).

Major dissolved gases in the stream—The responses of major dissolved gases (Ar and N_2) to changing equilibrium states were used in the evaluation of gas transfers including ^{15}N-enriched N_2 during the tracer experiment. Concentrations of Ar and N_2 increased simultaneously at all collection sites as gas solubilities increased with decreasing temperature (Fig. 6). On average, the N_2 : Ar ratios measured by GC were elevated slightly with respect to air-saturated water (Fig. 7a), which could indicate minor but variable components of either excess N_2 (e.g., from denitrification) or excess air (e.g., from solution of bubbles). If the samples had no excess air, the data would indicate excess N_2 concentrations averaging around 10 ± 10 μmol L^{-1}. Alternatively, if the samples had no measurable excess N_2, the data would indicate excess air concentrations of around 0.5 ± 0.5 cm^3 at standard temperature and pressure (ccSTP L^{-1}). These quantities are close to the limits of detection given the uncertainties of the GC analyses, and it is not clear whether they are real or artificial. Despite these uncertainties, it appears that the average rates of change of the Ar and N_2 concentrations were somewhat less than the rates of change of the equilibrium concentrations as a result of gas-transfer limitations.

In contrast, the concentrations of O_2 and CH_4 exhibited much larger deviations from air-saturation values (Fig. 6) and indicate changes in the redox status of the stream system. O_2 concentrations decreased simultaneously at all collection sites from about 115% of saturation at 1420 h to about 40% of saturation at midnight, presumably as a result of a decreasing ratio of photosynthesis : respiration with de-

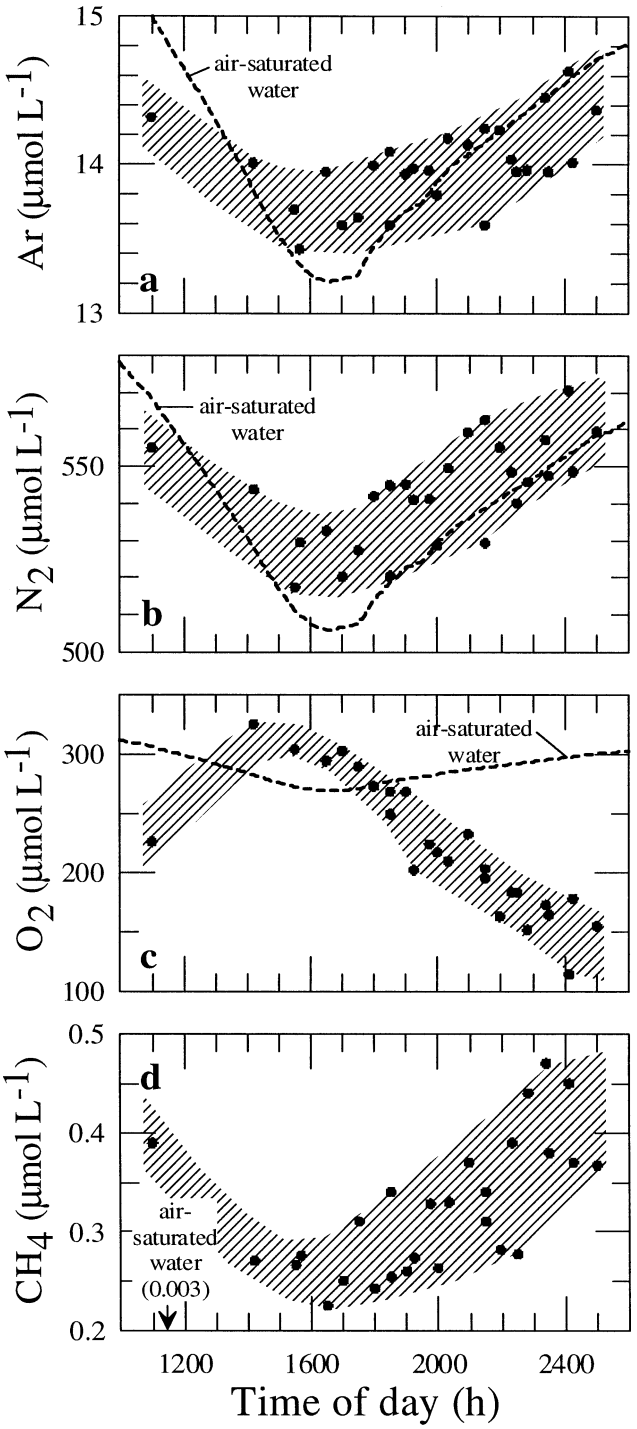

Fig. 6. Concentrations of Ar, N_2, O_2, and CH_4 in the stream. Dotted curves indicate atmospheric equilibrium concentrations calculated from the temperature record (Fig. 3). Shaded areas highlight trends inferred from the data.

creasing light intensity. During the same period, CH_4 concentrations remained highly supersaturated and increased on average from about 250 to 400 nmol L^{-1} (Fig. 6).

Nitrogen gas isotopes in the stream—Changes in $\delta^{15}N[N_2]$ at all five collection sites provide unequivocal evidence for

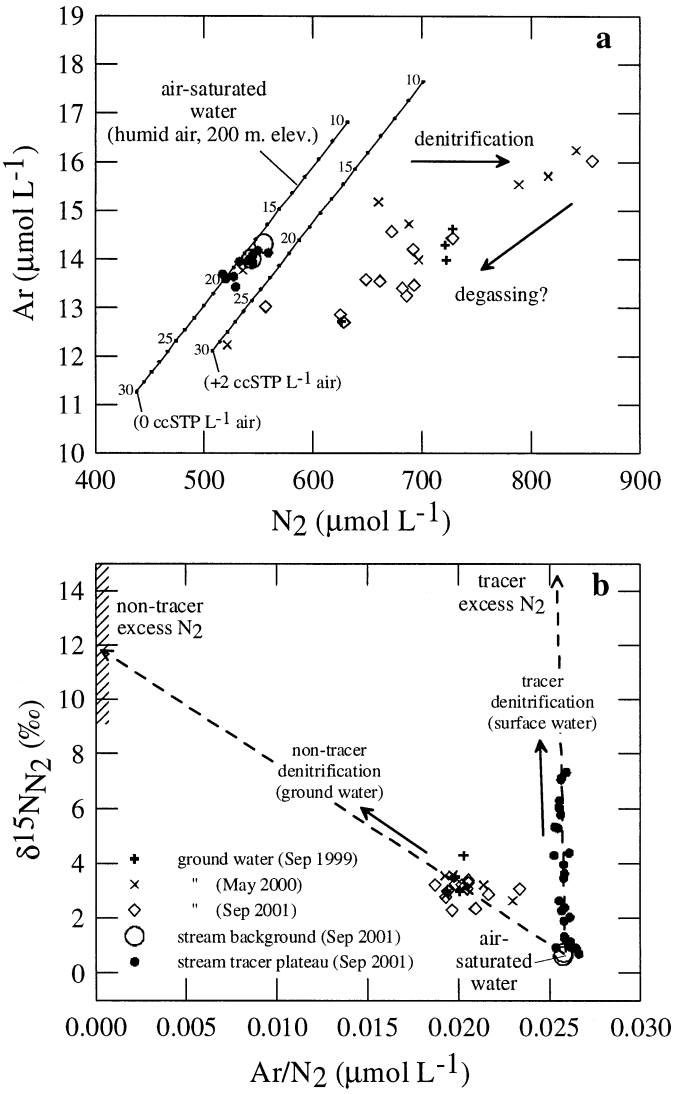

Fig. 7. Concentrations of Ar, N_2, and $\delta^{15}N[N_2]$ values in stream water and in groundwater from beneath the stream. (a) Curves indicate concentrations in equilibrium with air at 200 m elevation and 100% relative humidity, with 0 or 2 ccSTP L^{-1} of excess unfractionated air, at temperatures ranging from 10°C to 30°C. (b) Non-tracer groundwaters beneath the stream have large amounts of excess N_2 with only slightly elevated $\delta^{15}N[N_2]$, whereas stream tracer plateau samples have small amounts of excess N_2 with much higher $\delta^{15}N[N_2]$.

denitrification of tracer NO_3^- (Figs. 7b, 8). Values of $\delta^{15}N[N_2]$ range from the equilibrium air-saturation value (+0.7‰) in the background samples to as high as +7‰ during the passage of the tracer at sites D and E.

Values of $\delta^{15}N[N_2]$ increased systematically going downstream, and they increased with time at each site. Downstream intersite increases are consistent with progressive tracer denitrification with limited atmospheric exchange and can be related to the reach-scale denitrification rate. However, the temporal intrasite increases indicate that the transfer of tracer ^{15}N from NO_3^- to N_2 may not have been at steady state in the early parts of the tracer plateau. Delays in the ^{15}N transfer could have been caused by delayed transport of

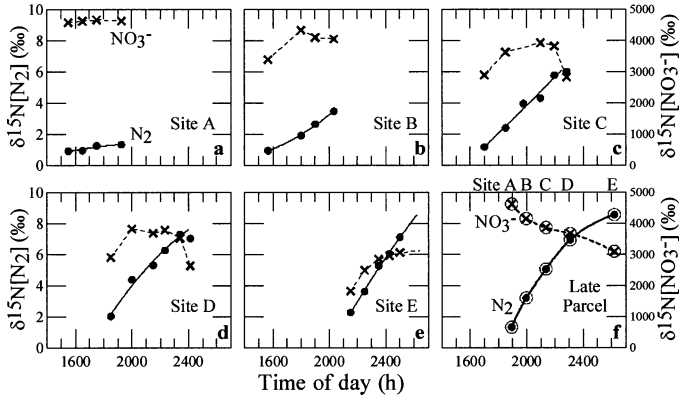

Fig. 8. Variation of $\delta^{15}N[N_2]$ and $\delta^{15}N[NO_3^-]$ values in the stream during the passage of the tracer. (a–e) Measured values at tracer sample sites A to E. (f) Estimated values for a hypothetical parcel of stream water that passed the injection site at 1830 h and moved downstream with the late part of the tracer plateau. The $\delta^{15}N[NO_3^-]$ values of this parcel are plateau averages (sites A to D) or the highest measured value (site E). The $\delta^{15}N[N_2]$ values of this parcel were estimated by interpolating or extrapolating from the data in panels a–e, using the travel times from Table 1. The values in panel f are the target values for the reaction simulations (*see Fig. 9*).

tracer NO_3^- to reaction sites or by reservoirs of intermediate species in the reaction sequence such as NO_2^- or N_2O. Alternatively, the intrasite increases in $\delta^{15}N[N_2]$ could indicate that reaction rates increased during the experiment or that gas-transfer velocities decreased during the experiment. The $\delta^{15}N[N_2]$ values appear to have leveled off or decreased slightly near the end of the tracer plateau at sites A and D, especially when $^{15}N[NO_3^-]$ values decreased (site D). These observations indicate that the response times of $\delta^{15}N[NO_3^-]$ and $\delta^{15}N[N_2]$ may have been similar enough that the $\delta^{15}N[N_2]$ values were close to steady state by the end of the tracer plateau and would be consistent with the relatively short average storage residence times indicated by the Br breakthrough curves (Table 1). In any case, it is concluded that steady-state reaction simulations are more likely to match $\delta^{15}N[N_2]$ observations near the end of the tracer plateau than near the beginning of the plateau. The flux of tracer $^{15}N_2$ near the end of the tracer plateau at each site was calculated from an appropriate version of Eq. 7. This tracer $^{15}N_2$ flux increased systematically between sites A and E by at least 1.4 μmol s^{-1} (as N).

Nitrite and nitrous oxide in the stream—Intermediate species in the denitrification reaction (NO_2^- and N_2O) were considered as potential reservoirs of tracer ^{15}N that could have affected the rate at which ^{15}N was transferred from NO_3^- to N_2. During the tracer plateau, the average concentration of NO_2^- was 3.0 ± 1.0 μmol L^{-1} ($NO_3^-:NO_2^- = 23$). These concentrations are high enough that NO_2^- could have been an important reservoir of tracer ^{15}N if it were an intermediate species in the tracer denitrification. Four samples from the late parts of the tracer plateau at sites D and E yielded average $\delta^{15}N[NO_2^-]$ values of approximately +300‰ to +350‰, significantly higher than a single value from site A (+30‰; Fig. 5). Allowing for 0–1% potential cross-contamination by tracer NO_3^- in the NO_2^- eluted from the SPE column (based on experiments with reference solutions), the fraction of the surface-water NO_2^- that was produced by denitrification of tracer NO_3^- may have ranged from about 0 to as much as 10%. The flux of tracer $^{15}NO_2^-$ increased between sites A and E by about 0.17 μmol s^{-1}, and the corresponding rate of total NO_2^- production is about 0.04 μmol L^{-1} h^{-1}. This rate of NO_2^- production is small in comparison to the rates of NO_3^- loss and N_2-N production and indicates that most of the NO_2^- in the stream was produced by a process other than denitrification of tracer NO_3^-. Nevertheless, even if the bulk of the NO_2^- was not formed by denitrification of tracer NO_3^-, it is considered to be a component of the stream N oxide pool being denitrified further to N_2.

Concentrations of N_2O in the stream before and during the tracer plateau were between about 20 and 30 nmol L^{-1} (R.L. Smith unpubl. data). These concentrations are about 2–3 times air-saturation values and indicate a minor source of N_2O such as nitrification or denitrification; however, they are two orders of magnitude lower than the NO_2^- concentrations and indicate that N_2O was not a significant reservoir of tracer ^{15}N in the stream.

Suspended particulate nitrogen—Suspended particulate N was analyzed to determine whether direct assimilation by planktonic or suspended benthic organisms was a sink for tracer $^{15}NO_3^-$. Eleven samples of suspended material collected during the tracer plateau at sites A, D, and E yielded an average particulate N concentration of 4.1 ± 0.5 μmol L^{-1} and $\delta^{15}N$ values ranging from +7‰ to +13‰ (Fig. 5), similar to the range of normal background values (Tobias unpubl. data) and with no systematic downstream trend. The maximum rate of tracer NO_3^- assimilation permitted by this range of $\delta^{15}N$ values (i.e., a maximum possible increase of 6‰ between sites I and A) would be of the order of 0.01 μmol L^{-1} h^{-1}, which is small in comparison to the rate of $^{15}NO_3^-$ loss. These data indicate that direct incorporation into the suspended material was not an important NO_3^- sink, but they do not rule out a more important role for benthic assimilation.

Characteristics of discharging groundwater—The origin and composition of groundwater discharge were evaluated because of the potentially important effects discharge may have on the benthic fluxes of NO_3^-, Ar, and N_2 and consequently on the determination of reach-scale reaction rates. Measured water-level gradients beneath the streambed indicate that some of the discharge was upward seepage through the bed sediments, but some also may have been lateral seepage through the stream banks.

Potential groundwater sources of NO_3^- include lateral seepage from shallow oxic or suboxic parts of the aquifer and nitrification of NH_4^+ in discharge from deeper reduced pore waters. Lateral seepage was not sampled directly, but is represented in part by discharge from active subsurface water-table drains. Two drainpipes within the tracer reach that were flowing in September 2001 had NO_3^- concentrations of 29 and 98 μmol L^{-1} with $\delta^{15}N[NO_3^-]$ values of +12.0‰ and +6.5‰, respectively. Other subsurface drains

to Sugar Creek had NO_3^- concentrations ranging from 190 to 440 μmol L^{-1} with $\delta^{15}N[NO_3^-]$ values between +8‰ and +21‰. In contrast, the available data indicate that discharging deep groundwater (from >0.3 m beneath the stream) was not a direct source of NO_3^-. Concentrations of NO_3^- and O_2 decreased downward to undetectable values at depths between about 0.03 and 0.3 m in most pore-water profiles sampled beneath Sugar Creek, which indicates that NO_3^- beneath the stream was derived locally, either from the stream or from in situ nitrification in the hyporheic zone, and was not a major constituent of the upwelling deep groundwater. Nitrification in upwelling groundwater may be important because deep groundwater sampled 0.3 to 1.5 m beneath gaining reaches of Sugar Creek at various times had NH_4^+ concentrations ranging from <1 to 200 μmol L^{-1}. Four samples with >30 μmol L^{-1} had $\delta^{15}N[NH_4^+]$ = +7.8‰ to +9.2‰ (average +8.4‰ [±0.5‰]). NO_3^- formed by nitrification of this groundwater NH_4^+ is likely to have $\delta^{15}N$ values around +8‰ to +9‰ or lower. Limited data indicate concentrations of NO_2^- ≤80 nmol L^{-1} and N_2O ≤ 2 nmol L^{-1} in deep groundwater beneath parts of Sugar Creek (R.L. Smith unpubl. data); however, the concentrations of these species in shallower groundwater, including the hyporheic zone, have not been documented.

Discharging deep groundwater is a potentially important source of excess nontracer N_2 and possibly Ar in the stream. Deep groundwater samples (0.3–1.5 m below the streambed) in gaining reaches of Sugar Creek, including the tracer reach, had relatively high N_2 : Ar ratios and variable Ar concentrations in comparison to the stream values (Fig. 7). Assuming little or no excess air, the concentrations of excess N_2 attributable to denitrification in these samples ranged from about 60 to 250 μmol L^{-1} (Fig. 7a). Independently of the isotope tracer experiment, $\delta^{15}N[N_2]$ values in these groundwaters ranged from +2.3‰ to +4.3‰ (average of about +3.3‰). Because these samples had no measurable NO_3^-, the gas data are interpreted to indicate complete denitrification of normal (nontracer) NO_3^- in local groundwater or surface water in which the initial NO_3^- before denitrification had an average $\delta^{15}N[NO_3^-]$ value given by that of the excess N_2 endmember (+12‰ [±3‰]; Fig. 7b).

The initial NO_3^- concentrations in the deep groundwaters beneath the stream (120–500 μmol L^{-1}) were higher than the stream NO_3^- concentrations in September 2001 (60–70 μmol L^{-1}). In addition, some of the groundwater samples had slightly higher Ar concentrations than surface waters at the corresponding collection times, consistent with recharge under cooler average conditions. Much of this deep groundwater probably was recharged beneath the land surface with NO_3^- from agricultural soils and was denitrified within the aquifer upgradient from the discharge area (Böhlke et al. 2002), although it is possible that some of these samples represent infiltrated stream water with relatively long residence times (2–3 months or more) in the hyporheic zone. In either case, the upwelling groundwaters are potentially important sources of nontracer excess N_2 that need to be included in the reaction model.

Simulation of nitrogen transformations and fluxes—The forward time-stepping reaction model for the reach-scale ^{15}N tracer experiment includes provision for nitrification, denitrification, assimilation (NO_3^- removal by processes other than denitrification), air–water gas exchange, and groundwater discharge. Denitrification and other processes affecting N_2 gas fluxes are a major focus of the simulations because of the importance of N_2 as a permanent sink for reactive N in aquatic systems. O_2 reduction is included because of its potential relation to nitrification and denitrification. To facilitate comparisons, fluxes and reaction rates are expressed as μmol m^{-2} h^{-1}, although some of these processes are not known to be limited to the benthos.

Representative reaction simulations are summarized in Table 3 and Fig. 9. For Br, NO_3^-, $\delta^{15}N[NO_3^-]$, and $\delta^{15}N[N_2]$, simulated values are compared to those of a parcel of stream water as it moved downstream past each of the collection sites (Table 2; Fig. 9). For Br, NO_3^-, and $\delta^{15}N[NO_3^-]$, the target stream value at each site is the average of the measured plateau values at the site, which could be assumed to be near steady state. In contrast, the $\delta^{15}N[N_2]$ values in the stream did not reach steady state at most sites by the end of the tracer Br and $^{15}NO_3^-$ plateau (Fig. 8f). To minimize potential transient effects of intermediate N pools, transport storage reservoirs, or changes in wind and light conditions on the calculations, the value of $\delta^{15}N[N_2]$ at each site in Fig. 9 is the interpolated or extrapolated value of a parcel that passed the injection site at 1830 h, near the end of the tracer plateau. The downstream evolution of this parcel is shown in Fig. 8f.

Because of ambiguity about the source of nontracer NO_3^- (nitrification or groundwater discharge), two contrasting assumptions about the composition of the groundwater discharge were evaluated: (1) discharging groundwater contained NO_3^-, as did the water flowing from identified drainpipes, and (2) discharging groundwater was completely denitrified and contained excess N_2, as did the samples collected 0.3–1.5 m below the stream bottom. The true average composition of discharge probably was between these extremes.

Simulations also were done with a range of gas-transfer velocities, some of which included variations with time. Given an average stream tracer velocity of about 0.04 m s^{-1}, channel depth of 0.19 m, and temperature of 18°C, the empirical relations of Bennett and Rathbun (1972; eqs. 104 and 165) yield a value of 0.04 m h^{-1} for GTV_{600}. However, the recorded change in average wind speed at Lafayette (from 6 to 2 m s^{-1}; Fig. 3) may indicate a substantial change in the values of GTV_{600} during the experiment, since values of GTV_{600} commonly increase rapidly at wind speeds higher than about 2 to 4 m s^{-1} (Wanninkhof et al. 1985; Donelan and Wanninkhof 2002). Although Sugar Creek is protected in part by steep banks, variations in wind speed at Lafayette, Indiana, have been shown to be correlated with variations in GTV_{600} in this watershed (Laursen and Seitzinger 2002; Laursen unpubl. data). Based on this correlation (derived from previous dual-gas tracer experiments), values of GTV_{600} decreased from around 0.2 m h^{-1} to 0.02 m h^{-1}, with an average of about 0.04 m h^{-1} between 1830 h (near the end of the injection period) and 2600 h (near the end of the collection period).

Plateau stream values of Br, NO_3^-, $\delta^{15}N[NO_3^-]$, and

Table 3. Selected simulation parameters for the reaction model.

Simulation*	**1**	1(−)	1(+)	2	3	4	**5**	5(−)	5(+)	6	7	8
GTV_{600} (m h^{-1})†	**wind**	wind	wind	0.00	0.03	0.06	**wind**	wind	wind	0.00	0.03	0.06
Ground water (BFG)‡	**denit**	denit	denit	denit	denit	denit	**+NO_3^-**	+NO_3^-	+NO_3^-	+NO_3^-	+NO_3^-	+NO_3^-
N_2-N (μmol L^{-1})	**1300**	1300	1300	1300	1300	1300	**1070**	1070	1070	1070	1070	1070
$\delta^{15}N[N_2]$ (‰)	**3.3**	3.3	3.3	3.3	3.3	3.3	**0.7**	0.7	0.7	0.7	0.7	0.7
NO_3^- (μmol L^{-1})	**0**	0	0	0	0	0	**115**	95	135	115	115	115
Denitrification (BFD)												
N_2-N (μmol m^{-2} h^{-1})	**120**	120	120	75	105	140	**125**	125	125	75	105	145
Assimilation (BFA)§												
NO_3^- (μmol m^{-2} h^{-1})	**100**	0	200	145	115	80	**95**	0	195	145	115	75
Nitrification (BFN)‖												
NO_3^- (μmol m^{-2} h^{-1})	**600**	500	700	600	600	600	**0**	0	0	0	0	0
O_2 Consumption (net)												
O_2-O (μmol m^{-2} h^{-1})	**13,000**	13,000	13,000	5000	10,000	16,000	**13,000**	13,000	13,000	5000	10,000	16,000

* Representative reaction simulations for a range of conditions in the tracer reach (*see Fig. 9*). Columns 1 and 5 (bold) are preferred alternatives. All simulations employ the same constant values of groundwater discharge (5.2 L m^2 h^{-1}) and groundwater Ar concentration (14.0 μmol L^{-1}). All simulations except the ones labeled (−) and (+) have NO_3^- total loss rates of 220 μmol m^{-2} h^{-1} (Fig. 9d) and all pass through the plateau $\delta^{15}N[N_2]$ value at site D (Fig. 9e).

† Wind indicates simulations in which GTV_{600} varies with wind speed (*see text*).

‡ Denit refers to discharge of denitrified groundwater containing excess N_2; +NO_3 refers to discharge of groundwater containing NO_3^- (assumed to have $\delta^{15}N[NO_3^-] = +20‰$).

§ Assimilation is defined as the difference between total NO_3^- loss and denitrification.

‖ NO_3^- formed by nitrification is assumed to have $\delta^{15}N[NO_3] = +8‰$.

$\delta^{15}N[N_2]$ were bracketed by simulations with benthic denitrification rates between 75 and 145 μmol m^{-2} h^{-1}, NO_3^- total loss rates between 120 and 320 μmol m^{-2} h^{-1}, and with addition of nontracer NO_3^- at rates between 500 and 700 μmol m^{-2} h^{-1} (Table 3; Fig. 9). Our preferred estimate of the rate of denitrification is about 120 ± 20 μmol m^{-2} h^{-1}, which would yield assimilation rates between about 0 and 200 μmol m^{-2} h^{-1} when subtracted from the total NO_3^- loss rates. The relatively large uncertainty given for assimilation (and total loss) is attributed in part to the high overall NO_3^- load and high rate of input of new NO_3^-, in comparison to which NO_3^- losses are relatively small. Some potential biases in the match between simulations and data also result from possible incomplete mixing at site A (Fig. 4), the discontinuity caused by the point source between sites A and B, and the incomplete plateau at site E (arrows in Fig. 9c,e). Focusing on the reach between sites B and D would yield a total NO_3^- loss rate between about 120 and 220 μmol m^{-2} h^{-1}, which indicates that denitrification was the dominant process of NO_3^- removal, with assimilation between about 0 and 100 μmol m^{-2} h^{-1}. The benthic denitrification flux alone corresponds to a first-order rate constant of about 0.009 h^{-1} or a zero-order NO_3^- loss rate of about 0.63 μmol L^{-1} h^{-1}. As illustrated in Fig. 9d,e, the combined effects of reactions and groundwater dilution would have caused about a 30% decrease in the NO_3^- concentration within the reach in the absence of NO_3^- sources.

For Ar and N_2 concentrations, selected simulation results are shown in comparison to all measured stream values (Fig. 9a,b) because the fluxes are not related to the presence or absence of the isotope tracer. The simulated Ar and N_2 concentrations tend to be slightly lower than the measured concentrations, but they bracket the measured rates of change. The simulated N_2 concentrations increase as a result of decreasing temperature, discharge of denitrified groundwater containing excess N_2, and denitrification. In simulations that include discharge of denitrified groundwater, the benthic flux of excess N_2 attributable to groundwater discharge (5–7 μmol m^{-2} h^{-1} as N) is an order of magnitude larger than the flux attributable to denitrification (0.6 μmol m^{-2} h^{-1} as N), so these simulations have substantially higher N_2 concentrations (by about 5–15 μmol L^{-1}) than simulations with undenitrified groundwater discharge (Fig. 9b). For both types of groundwater input, when GTV_{600} varies with wind speed, the N_2 flux attributed to denitrification is smaller than the flux attributed to air exchange (1–4 μmol m^{-2} h^{-1} as N with denitrified groundwater discharge; 4–8 μmol m^{-2} h^{-1} as N with undenitrified groundwater discharge). These calculations indicate that the effect of denitrification on the concentration of N_2 in the stream is small and would be difficult to detect in the absence of the isotope tracer. The simulations illustrate the potential for measurements of stream N_2 saturation states to yield unrealistically high estimates of benthic denitrification in some areas where groundwater discharge is important and not accounted for (*see also* Laursen and Seitzinger 2002).

Simulations in which GTV_{600} decreased with time in relation to decreasing wind speed generally provide better overall fits to the changes in Ar and N_2 concentrations and $\delta^{15}N[N_2]$ values than do simulations in which GTV_{600} had

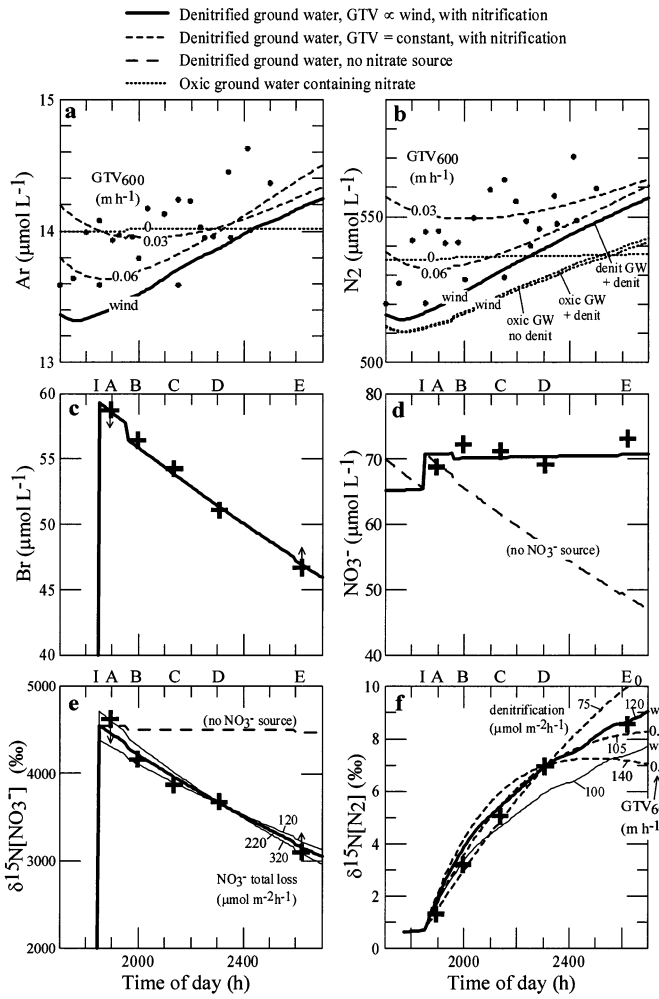

Fig. 9. Comparison of measured and simulated values of Ar, N_2, Br, NO_3^-, $\delta^{15}N[NO_3^-]$, and $\delta^{15}N[N_2]$ in a stream parcel traversing the tracer reach during the late part of the tracer plateau. Crosses indicate averaged or interpolated values for sites A to E, based on measurements during the tracer plateau (Table 2; Fig. 8f). The curves indicate simulation results for different sets of model parameters (Table 3). The heavy solid curve represents the preferred model with parameters given in Table 3, column 1. (a–b) Concentrations of Ar and N_2 were simulated using values of GTV_{600} that were constant (dashed lines labeled with GTV_{600} in m h^{-1}) or that varied with wind speed according to a local correlation (solid lines labeled wind). Small symbols indicate measured concentrations in all stream samples. (c) All models used a single constant value for groundwater discharge (BFG), yielding the solid curve. Small arrows indicate possible uncertainties in the data related to mixing and travel time at site A and approach to plateau at site E. (d) All models used the same balance between NO_3^- sources and sinks yielding relatively constant NO_3^- concentration (solid line) except for a sensitivity test in which sources were removed (dashed line). (e) Curves passing through the measured value at site D illustrate a range of NO_3^- total loss rates; large uncertainties in these rates are a result of high overall NO_3^- fluxes, uncertainties in the isotope analyses, and potential biases in the data at sites A and E (small arrows). (f) Simulations for constant and varying GTV_{600} are illustrated as in panel a. The model with GTV_{600} = 0.03 m h^{-1} and BFD = 100 μmol m^{-2} h^{-1} (dashed) is similar to the model with GTV_{600} varying and BFD = 120 μmol m^{-2} h^{-1} (solid). For models with varying GTV_{600}, earlier measurements could be fit with a slightly lower value of BFD than later measurements (solid lines).

constant values (Fig. 9a,b,f). Among the simulations with constant values of GTV_{600}, the one with GTV_{600} = 0.03 m h^{-1} (consistent with the equations of Bennett and Rathbun 1972) gives a good match for $\delta^{15}N[N_2]$ but not so good for Ar and N_2 concentrations. Results for GTV_{600} values of 0 and 0.06 m h^{-1} appear to be out of range. For GTV_{600} = 0.03 m h^{-1}, the simulation indicates that $\delta^{15}N[N_2]$ should have stopped increasing with distance downstream beyond site E as the rates of production and exchange of tracer-derived N_2 reached a steady state. At higher values of GTV_{600}, steady-state $\delta^{15}N[N_2]$ values would have occurred earlier (e.g., after about 6 h for GTV_{600} = 0.06). From these comparisons, it appears that the length of the tracer reach from site A to site E probably was close to giving the maximum possible $\delta^{15}N[N_2]$ signal given the denitrification rate and gas-transfer conditions at the time.

Potential effects of NO_2^- on the ^{15}N tracer results were evaluated by assuming all the NO_2^- was formed by denitrification of tracer NO_3^- and had a steady-state concentration of 3 μmol L^{-1}. These results (not shown) indicate that the $\delta^{15}N$ value of the NO_2^- should have reached a value about half that of the coexisting NO_3^- by site C and approximately equal to the NO_3^- value by site E if the NO_2^- was an intermediate species in denitrification of surface-water NO_3^- leading to the ^{15}N enrichment of the N_2. Because the $\delta^{15}N$ values of the NO_2^- remained low throughout the reach (Fig. 5), the simulations confirm that the bulk of the NO_2^- in the stream was formed by some process other than denitrification of the surface-water NO_3^-.

The relatively high concentration of NO_2^- in the stream and the relative absence of tracer ^{15}N in the NO_2^- indicate that nitrification may have been an important source of NO_2^- and possibly of nontracer NO_3^- contributing to the increase in the NO_3^- load. The maximum rate of nitrification estimated from the reach-scale tracer experiment (600 ± 100 μmol m^{-2} h^{-1} if groundwater discharge contained no NO_3^-) would be balanced stoichiometrically by reduction of 1,200 μmol m^{-2} h^{-1} of O_2, which is about 18% of the estimated reach-scale rate of O_2 consumption (6,500 μmol m^{-2} h^{-1}; Table 3). This ratio of nitrification : O_2 reduction is within the range reported for benthic processes in some other freshwater systems (Hall and Jeffries 1984; Jensen et al. 1994), but it could be considerably lower if NO_3^- was added with groundwater discharge.

Discussion

There are few established methods for estimating denitrification in streams and rivers that reliably integrate spatial variation and resolve denitrification from other reactions that affect NO_3^- mass balances. The $^{15}NO_3^-$ injection method addresses these concerns through reach-scale averaging and monitoring of the specific product ($^{15}N_2$) of the denitrification of labeled in-stream NO_3^-. In particular, the reach-scale averaging afforded by the method addresses the specific need for scaling up observations to a level appropriate for water-quality investigations and eventual development of improved agricultural best management practices that increase protection for receiving waters. The $^{15}NO_3^-$ injection method is not

without its uncertainties and needs for improvement. This discussion addresses a number of outstanding technical issues and also compares our results with those recently obtained with similar methods as well as some previous assessments of the importance of in-stream denitrification.

Isotope tracer method—The design of our $^{15}NO_3^-$ tracer experiment included the following considerations: (1) stream NO_3^- concentrations should be left relatively unaltered so that subsurface chemical gradients and reaction rates are not changed substantially; (2) the ^{15}N concentration of the NO_3^- should be high enough to produce a measurable change in the $\delta^{15}N$ value of total dissolved N_2 after a few hours of downstream transport; (3) the tracer concentrations should be maintained at a steady state in the stream long enough for quasi–steady-state conditions to be established in the major reaction sites including the hyporheic zone. Results indicate that these major objectives were largely met and that the isotope tracer permitted measurement of denitrification in a gaining stream that would be undetectable from chemical mass-balance approaches.

Compared to methods that derive denitrification rates from N_2 gas-saturation states, the isotope method can be more sensitive, yielding measurable denitrification rates in some cases where the gas-transfer rates would be too high to permit measurable gas supersaturations, even with high-precision measurements (Laursen and Seitzinger 2002). The isotope approach may be important especially in reaches where groundwater discharge is a major source of N_2 supersaturation. Our simulations indicate that the increase in concentration of N_2 caused by denitrification may have been less than 10% of the increase caused by discharge of previously denitrified groundwater in the gaining tracer reach of Sugar Creek.

The relatively low level of isotopic enrichment used in this study (2% ^{15}N) has some advantages over the severe enrichments (>50% ^{15}N) used in some other isotopic tracer studies of denitrification. High-level enrichment experiments have the potential for detecting coupled nitrification–denitrification from nonequilibrated distributions of $^{14}N^{14}N$, $^{14}N^{15}N$, and $^{15}N^{15}N$ molecules (Nielsen 1992). But high-level isotope enrichments require substantial increases in the total NO_3^- concentration, which could affect the processes being measured. Specifically, higher concentrations of NO_3^- can stimulate substrate-limited reactions, resulting in enhanced rates and(or) shifts in the relative importance of competing reaction pathways. Low-level isotope enrichment experiments can be done with minimal change in the chemical composition of the system, and some of the effects of nitrification can be estimated indirectly. However, we have not addressed nitrification directly in this study, and we do not know whether NO_3^- assimilation might have yielded measurable ^{15}N enrichment in benthic organisms or sediments, which were not analyzed.

The reaction simulation scheme used here differs somewhat from other representations of stream nutrient spiraling used in previous studies. Commonly, steady-state first-order reaction rate constants (k) and corresponding mean travel distances (S_w) are derived directly from measurements with respect to distance along the stream (Newbold et al. 1981; Stream Solute Workshop 1990; Peterson et al. 2001). As illustrated below, our forward time-stepping approach is consistent and compatible with the spiraling approach in certain situations. We believe it also has important advantages for some purposes: (1) temporal variations in temperature, gas transfer, reaction rates, and other variables can be incorporated at diel and other time scales in simulations of non–steady-state conditions; (2) rates are derived with respect to time and normalized with respect to sediment–water interface area, which are more directly comparable with other types of laboratory and field data; (3) processes such as nitrification, groundwater discharge, and gas fluxes can be treated explicitly along with denitrification and assimilation, providing simulations for a large number of measured quantities (e.g., Fig. 9); (4) intermediate reaction species such as NO_2^- and N_2O can be integrated with the isotope transfer calculations; (5) point sources such as tributaries and drains and spatial variations in processes such as groundwater inputs can be incorporated. We have not addressed all of these features in the current study, but we expect they will be important as studies of this type evolve.

Experimental uncertainties—While demonstrating some of the capabilities of the isotope tracer approach, this study also exposes some questions that require further work. For example, with respect to denitrification: (1) What are the major sources of uncertainty and ambiguity in the derived rates? (2) What is the overall composition of groundwater discharge (e.g., denitrified or containing NO_3^-)? (3) What controls the rate at which stream $^{15}N_2$ values approach a steady state at a given site? (4) What is the effect of hidden nitrification in the hyporheic zone on the isotopic composition of NO_3^-, NO_2^-, N_2O, and N_2 at denitrification sites in the sediment pore waters? (5) Do reaction rates change measurably on the time scale of an experiment?

One limitation on the isotope tracer calculations leading to the denitrification rate is uncertainty and potential variability of the gas-transfer velocities. Sensitivity tests indicate that the calculation may not be particularly sensitive to this within reasonable limits established by local gas tracer studies, but further work on this is in progress. The uncertainties of the isotopic analyses of N_2 are essentially insignificant, and the estimation of the denitrification rate from the N_2 isotope data is largely unaffected by uncertainties in the NO_3^- mass balance. In contrast, the isotope mass-balance calculations leading to the rate of NO_3^- uptake by processes other than denitrification (e.g., assimilation) are relatively imprecise because of the high NO_3^- fluxes (small relative net losses) and high rates of NO_3^- additions in the tracer reach at Sugar Creek. These limitations may be expected to apply to other similar studies in agricultural watersheds. Nevertheless, the denitrification rate is important by itself because denitrification removes NO_3^- from the potentially reactive N pool in the stream system, whereas assimilation does not.

An important ambiguity in the tracer simulations arises from uncertainty about the composition of groundwater discharge and its consequent effect on estimated nitrification rates. If discharge were dominated by upwelling N_2-rich (NO_3^--free) groundwater, then the tracer results would require a substantial source of unlabeled NO_3^- such as nitrifi-

cation at a rate of about 600 μmol m^{-2} h^{-1} (Table 3). Alternatively, the tracer data could be accounted for in the absence of nitrification by lateral seepage containing around 100–135 μmol L^{-1} NO_3^-. Both types of groundwater have been identified in the vicinity of the tracer reach. It is almost certain that the deep groundwater is a component of the discharge, but the relative discharge rates of the two types are difficult to quantify. Nevertheless, although uncertainty about the average composition of the discharge causes large uncertainty with respect to the nitrification rate, this source of uncertainty does not have a significant effect on the simulated denitrification rate, nor would it necessarily have a major effect on the inferred total N budget of the stream system.

More data also are needed to demonstrate conclusively that $\delta^{15}N[NO_3^-]$ achieved a steady state at the major sites of denitrification. If not, then the rates of denitrification would be underestimated by calculations based on $\delta^{15}N[NO_3^-]$ and $\delta^{15}N[N_2]$ in the stream. Various types of evidence indicate that nontracer NO_3^- was largely, if not completely, replaced by tracer NO_3^- by the end of the experiment. For example, at site A, $\delta^{15}N[N_2]$ in the stream appears to have leveled off by the end of the $\delta^{15}N[NO_3^-]$ plateau. At site D, $\delta^{15}N[N_2]$ began to decrease soon after $\delta^{15}N[NO_3^-]$ decreased. These preliminary observations indicate that the isotopic compositions of the reactant and product at the main reaction sites both responded to changes in the surface water on time scales of the order of 1–3 h. In addition, pore-water data from beneath the stream indicate that, within the depth range of measurable NO_3^-, tracer Br profiles typically approach quasi–steady-state gradients within a few hours after tracer Br plateaus are achieved in the overlying surface water (Harvey unpubl. data). In a single profile at site A, Br-rich pore waters yielded $\delta^{15}N[NO_3^-]$ values approaching those of the stream tracer, with corresponding $\delta^{15}[N_2]$ values as high as +140‰. These observations provide qualitative evidence that tracer NO_3^- largely replaced nontracer NO_3^- at denitrification sites beneath the stream by the end of the tracer plateau in the stream, but the completeness and generality of this replacement are not known.

Having achieved steady state, the $\delta^{15}N[NO_3^-]$ values in denitrifying pore waters still might have been different from those in the stream if nitrification occurred in the subsurface and the nontracer NO_3^- produced there was denitrified before exchanging with surface-water NO_3^-. In this case, the rate of denitrification of the tracer NO_3^- calculated from the isotope data would be less than the total denitrification rate of the system.

Whereas the reaction rates were assumed to be constant in the reaction simulations, the timing of the experiment over the day–night transition and concomitant 50% decrease in O_2 concentration may indicate otherwise. Denitrification rates may be either positively or negatively correlated with O_2 concentrations, depending on the relative importance of nitrification as a source of NO_3^- for denitrification or of O_2 as an inhibitor of denitrification (Christensen et al. 1990; Risgaard-Petersen et al. 1994; An and Joye 2001; Kemp and Dodds 2002*b*). Other studies have indicated that coupled nitrification–denitrification may be relatively unimportant in systems with high NO_3^- concentrations (Christensen et al. 1990; Cornwell et al. 1999), but this has not been proved in Sugar Creek. Our data could be consistent with a modest increase in the rate of denitrification with decreasing O_2 during the course of the experiment (perhaps beginning around 100 μmol m^{-2} h^{-1}; Fig. 9f) but probably would not be consistent with a decrease in the rate. Similarly, because the simulated part of the experiment ran from around dusk to after midnight, it is possible that the rate of NO_3^- assimilation associated with photosynthesis decreased with time. Simulations with decreasing rates of assimilation would give good overall fits to the $^{15}NO_3^-$ fluxes and $\delta^{15}N[NO_3^-]$ values (Fig. 9e), but definitive evidence for these changes would require longer tracer injections.

Comparative rates of in-stream processes—Our results may be compared to other estimates of denitrification in streams, but differences in techniques can make such comparisons difficult in some cases. The reach-scale denitrification rate derived from the in-stream tracer is within the range of values derived from small-scale incubations with intact cores from Sugar Creek using high-precision gas measurements as well as isotope tracer techniques (M. A. Voytek et al. unpubl. data; L. K. Smith et al. unpubl. data). The reach-scale rate is approximately half the average value obtained from seven core sites within the tracer reach in September 2001 (L.K. Smith et al. unpubl. data). Differences between these methods include (1) core incubations do not permit hyporheic flow and (2) a composite of core incubation results may not represent the average stream result because some bottom types are overrepresented or underrepresented in the cores. In addition, a substantial source of uncertainty exists in the comparison of reach-scale and lab-scale benthic fluxes simply because of uncertainties in the composite depth and total area of the stream bottom within the reach.

Our results are substantially different from those of a similar reach-scale isotope tracer experiment conducted in Walker Branch, Tennessee (Mulholland et al. 2004; Table 4). The experimental reach at Walker Branch was in a forested watershed and had much smaller NO_3^- concentration and flux than Sugar Creek. To compare results of the two studies, we calculated rates of total NO_3^- loss and denitrification at Sugar Creek by two approaches: (1) our preferred simulation results, from Table 3, column 1, in μmol m^{-2} h^{-1}, were converted to units of NO_3^- uptake length (S_w), first-order loss rate (k), and vertical transfer velocity by using average values of stream depth, area, velocity, and NO_3^- concentration (Newbold et al. 1981; Stream Solute Workshop 1990) and (2) values of k and S_w were derived directly with respect to distance by fitting our data to simplified steady-state equations for the $^{15}NO_3^-$ and $^{15}N_2$ tracer fluxes (Mulholland et al. 2004) and then converted to vertical fluxes and transfer velocities (Table 4). The two calculation procedures are in reasonably good agreement at Sugar Creek, where different rate laws are difficult to distinguish because the fractional changes in stream tracer fluxes are relatively small.

Expressed as vertical fluxes (μmol m^{-2} h^{-1}) the total NO_3^- loss rate at Sugar Creek was about 2–3 times as high, and the denitrification rate was about 10 times as high, as the rates at Walker Branch. The fraction of NO_3^- loss attrib-

Table 4. Comparison of stream characteristics and NO_3^- cycling rates derived from $^{15}NO_3^-$ tracer studies in a high-NO_3^- stream in an agricultural watershed (Sugar Creek, Indiana; this study) and a low-NO_3^- stream in a forested watershed (Walker Branch, Tennessee; Mulholland et al. 2004).

	Sugar Creek*	Sugar Creek†	Walker Branch†‡
Average stream characteristics§			
Flow (L s^{-1})	45	45	0.4
Depth (m)	0.19	0.19	0.029
Effective area (m^2)	1.0	1.0	0.027
Solute velocity (m s^{-1})	0.043	0.043	0.015
NO_3^- concentration (μmol L^{-1})	71	71	1.9
NO_3^- flux (μmol s^{-1})	3200	3200	0.76
Reach-scale N transfers‖			
NO_3^- total loss, k_{tot} (m^{-1})	0.000105	**0.000104**	**0.028**
Denitrification, k_{den} (m^{-1})	0.000057	**0.000054**	**0.0046**
NO_3^- total loss, $S_{w,tot}$ (m)	9500	**9600**	**36**
Denitrification, $S_{w,den}$ (m)	17,400	**18,500**	**217**
NO_3^- total loss (m h^{-1})	**0.0031**	0.0031	0.044
Denitrification (m h^{-1})	**0.0017**	0.0016	0.0062
NO_3^- total loss (μmol m^{-2} h^{-1})	**220**	220	82
Denitrification (μmol m^{-2} h^{-1})	**120**	115	12

* Reaction rates were derived initially (bold type) as benthic fluxes (and benthic transfer velocities) using Eqs. 1–6 (this study) by trial-and-error fits to $^{15}NO_3^-$ and $^{15}N_2$ abundances with time-based, forward-stepping reaction simulations. Those results were converted subsequently (nonbold type) to first-order units with respect to distance using average stream parameters.

† Reaction rates and distances were derived initially (bold type) from fits to the distances and fluxes of tracer $^{15}NO_3^-$ and tracer $^{15}N_2$-N (sensu Newbold et al. 1981; Mulholland et al. 2004): tracer $^{15}NO_3^-$ flux = $(^{15}NO_3^-)^\circ\, e^{-k_{tot}x}$ and tracer $^{15}N_2$-N flux = $[k_{den}/(k_{gtv} - k_{tot})]\ (^{15}NO_3^-)^\circ\ (e^{-k_{tot}x} - e^{-k_{gtv}x})$, where k_{tot}, k_{den}, and k_{gtv} (in m^{-1}) are first-order rate constants for NO_3^- total loss, denitrification, and gas transfer, respectively; $(^{15}NO_3^-)^\circ$ is the tracer $^{15}NO_3^-$ flux at the upstream site; x (in m) is distance downstream, and the tracer fluxes are given by Eq. 7 and its equivalent for N_2-N. For this calculation, the value of k_{gtv} at Sugar Creek was assumed to be 0.0009 m^{-1}, which corresponds to a value of 0.03 m h^{-1} for GTV_{600}. Those results were converted subsequently (nonbold type) to benthic fluxes and benthic transfer velocities by using average stream parameters.

‡ Data in this column are from Mulholland et al. (2004).

§ Average values for the reach during the tracer experiment.

‖ k (downstream distance rate constant) and S_w (downstream mean travel distance) are stream-nutrient spiraling terms for first-order reactions (Newbold et al. 1981; Stream Solute Workshop 1990).

utable to denitrification was of the order of one half at Sugar Creek and only about 16% at Walker Branch. These comparisons could indicate that the rate of benthic denitrification was positively correlated with the NO_3^- concentration, whereas the rate of NO_3^- assimilation was less so, although other explanations are also possible. The first-order approximations of NO_3^- loss and denitrification with respect to stream distance are even more different between the two watersheds because the flow, velocity, depth, and NO_3^- concentration were also higher in Sugar Creek. Thus, the mean travel distance of NO_3^- in Walker Branch was roughly two orders of magnitude shorter than in Sugar Creek, even though the benthic fluxes were only different by about a factor of 2–3. These comparisons illustrate fundamental differences not only between the two streams but also between the different definitions of N losses in streams (e.g., reach-scale rate constants vs. vertical fluxes). For example, reaction rates expressed as vertical fluxes may be related relatively directly to other experimental data on the intrinsic reaction controls of NO_3^- losses in the benthos, such as the chemical and physical properties of the bed sediments and biota. Reach-scale rate constants embody not only the intrinsic reaction controls but also a number of additional site-specific variables such as stream size and chemical load that are needed to assess watershed mass balance. Both types of expression have value if the differences are recognized when results are compared.

Despite an overall increase in the stream NO_3^- load within our experimental reach, the rate of denitrification represented a substantial sink for N leaving the watershed. Nevertheless, the reach-scale rates of denitrification and NO_3^- loss, derived at a time of relatively low flow and low NO_3^- concentration in the stream, may not be sufficient to account for annual average N losses derived from some types of regional models and statistical studies. For example, our denitrification rate is equivalent to a vertical NO_3^- transfer velocity of 0.04 m d^{-1}, which is low in comparison to the range predicted for benthic denitrification in streams (0.05–0.14 m d^{-1}) according to data compiled by Howarth et al. (1996). First-order loss rates derived from spatial regression of total N loads and fluxes in major stream networks (Preston and Brakebill 1999; Alexander et al. 2000) would be roughly consistent with vertical transfer velocities of around 0.2–0.3 m d^{-1}, substantially higher than our total loss estimates, although other stream variables may interfere with this comparison. Regardless of how the rates are derived and expressed, it is emphasized that our tracer study does not represent winter and spring conditions in Sugar Creek, when stream flow, NO_3^- concentration, and NO_3^- flux are much higher. Unless the rates of NO_3^- uptake and denitrification increase proportionally with NO_3^- flux, the relative importance of NO_3 loss may be less in high flow conditions than it was during this experiment.

Summary—In summary, a reach-scale tracer test with $^{15}NO_3^-$ indicated that denitrification was a substantial sink for NO_3^- leaving a small agricultural watershed, and this sink would not have been detected from measurements of stream NO_3^- loads in the absence of the isotope tracer. The tracer experiment was conducted during low-flow conditions in a 1.2-km reach of a second-order stream with a NO_3^- concentration of 71 μmol L^{-1}. A forward time-stepping numerical scheme was used to simulate changes in a parcel of water as it moved downstream in the tracer cloud, subject to vertical fluxes of water and solutes across the air–water and sediment–water interfaces. Reach-scale average rates of denitrification, nitrification, assimilation, groundwater discharge, and gas exchange with air were determined by comparing simulation results with measurements of changes in Ar, N_2, Br, NO_3^-, $\delta^{15}N[NO_3^-]$, $\delta^{15}N[NO_2^-]$, and $\delta^{15}N[N_2]$ as the tracer cloud moved downstream, with the following results:

(1) A systematic increase in $\delta^{15}N[N_2]$ indicated denitrification of surface-water NO_3^- at a rate of about 120 ± 20 μmol m^{-2} h^{-1} (corresponding to about 0.63 μmol L^{-1} h^{-1} or 0.009 h^{-1}).

(2) A decrease in the flux of tracer $^{15}NO_3^-$ combined with the estimated denitrification rate indicated NO_3^- assimilation (or other unspecified loss) at a relatively uncertain rate between about 0 and 200 μmol m^{-2} h^{-1}, probably nearer the low end. Assimilation by suspended particulate matter was equivalent to 2 μmol m^{-2} h^{-1} or less, but benthic uptake was not assessed.

(3) A 25% increase in flow through the reach and little or no net change in NO_3^- concentration implied a substantial increase in the NO_3^- load, which indicates that NO_3^- loss by denitrification and assimilation was more than offset by NO_3^- addition.

(4) The rate of decrease in $\delta^{15}N[NO_3^-]$ indicated gross input of unlabeled NO_3^- was about 600 μmol m^{-2} h^{-1}. This input can be accounted for either by in-stream nitrification (if groundwater inputs were completely denitrified, as indicated by pore waters beneath the stream) or by NO_3^- inputs with groundwater inflow (if all groundwater inputs occurred as shallow lateral seepage with an average NO_3^- concentration of about 115 μmol L^{-1}).

(5) A minor increase in $\delta^{15}N[NO_2^-]$ indicated that about 10% of the NO_2^- in the stream was formed by denitrification of tracer NO_3^-, but most of the NO_2^- was produced by a process other than denitrification of the tracer NO_3^-, possibly by nitrification.

(6) The concentrations and fluxes of N_2 were dominated by the effects of changing temperature and groundwater discharge, whereas the flux of N_2 caused by denitrification was undetectable in the absence of the ^{15}N tracer.

Additional experiments are needed to assess benthic assimilation as a NO_3^- sink, to resolve local NO_3^- sources (including nitrification), and to determine how processes vary spatially, as functions of flow and NO_3^- concentration, and at various time scales (e.g., diel, seasonal). Reach-scale experiments in high-NO_3^- streams in agricultural watersheds such as this one are especially important for understanding controls on the large fluxes of N through major drainage systems like the Mississippi basin.

References

ALEXANDER, R. B., R. A. SMITH, AND G. E. SCHWARTZ. 2000. Effect of stream channel size on the delivery of nitrogen to the Gulf of Mexico. Nature **403:** 758–761.

AN, S. M., AND S. B. JOYE. 2001. Enhancement of coupled nitrification-denitrification by benthic photosynthesis in shallow estuarine sediments. Limnol. Oceanogr. **46:** 62–74.

BENNETT, J. P., AND R. E. RATHBUN. 1972. Reaeration in open-channel flow. U.S. Geological Survey Professional Paper 737.

BÖHLKE, J. K., AND T. B. COPLEN. 1995. Interlaboratory comparison of reference materials for nitrogen-isotope-ratio measurements, pp. 51–66. *In* Reference and intercomparison materials for stable isotopes of light elements, IAEA TECDOC 825. International Atomic Energy Agency.

———, C. J. GWINN, AND T. B. COPLEN. 1993. New reference materials for nitrogen-isotope-ratio measurements. Geostandards Newsl. **17:** 159–164.

———, R. WANTY, M. TUTTLE, G. DELIN, AND M. LANDON. 2002. Denitrification in the recharge area and discharge area of a transient agricultural nitrate plume in a glacial outwash sand aquifer, Minnesota. Water Resour. Res. **38:** 10.11 to 10.26.

CHRISTENSEN, P. B., L. P. NIELSEN, J. SORENSEN, AND N. P. REVSBECH. 1990. Denitrification in nitrate-rich streams: Diurnal and seasonal variation related to benthic oxygen metabolism. Limnol. Oceanogr. **35:** 640–651.

COPLEN, T. B., H. R. KROUSE, AND J. K. BÖHLKE. 1992. Reporting of nitrogen-isotope abundances. Pure Appl. Chem. **64:** 907–908.

CORNWELL, J. C., W. M. KEMP, AND T. M. KANA. 1999. Denitrification in coastal ecosystems: Methods, environmental controls, and ecosystem level controls, a review. Aquat. Ecol. **33:** 41–54.

DONELAN, M. A., AND R. WANNINKHOF. 2002. Gas transfer at water surfaces—concepts and issues, pp. 1–10. *In* M. A. Donelan, W. M. Drennan, E. S. Saltzman, and R. Wanninkhof [eds.], Gas transfer at water surfaces. American Geophysical Union, Geophysical Monograph 127.

GONFIANTINI, R. 1978. Standards for stable isotope measurements in natural compounds. Nature **271:** 534–536.

GOOLSBY, D. A., W. A. BATTAGLIN, B. T. AULENBACH, AND R. P. HOOPER. 2001. Nitrogen input to the Gulf of Mexico. J. Environ. Qual. **30:** 329–336.

HALL, G. H., AND C. JEFFRIES. 1984. The contribution of nitrification in the water column and profundal sediments to the total oxygen deficit of the hypolimnion of a mesotrophic lake (Grasmere, English Lake District). Microb. Ecol. **10:** 37–46.

HALL, R. O. J., AND J. L. TANK. 2003. Ecosystem metabolism controls nitrogen uptake in streams in Grand Teton National Park, Wyoming. Limnol. Oceanogr. **48:** 1120–1128.

HARVEY, J. W., AND B. J. WAGNER. 2000. Quantifying hydrologic interactions between streams and their subsurface hyporheic zones, pp. 3–44. *In* J. A. Jones and P. J. Mulholland [eds.], Streams and groundwaters. Academic.

HERBERT, R. A. 1999. Nitrogen cycling in coastal marine ecosystems. FEMS Microbiol. Rev. **23:** 563–590.

HOWARTH, R. W., AND OTHERS. 1996. Regional nitrogen budgets and riverine N and P fluxes for the drainages to the North Atlantic Ocean: Natural and human influences. Biogeochemistry **35:** 75–139.

HÜBNER, H. 1986. Isotope effects of nitrogen in the soil and biosphere, pp. 361–425. *In* P. Fritz and J. C. Fontes [eds.], Handbook of environmental geochemistry, volume 2, The terrestrial environment B. Elsevier.

JENSEN, K., N. P. SLOTH, N. RISGAARD-PETERSEN, S. RYSGAARD, AND N. P. REVSBECH. 1994. Estimation of nitrification and de-

nitrification from microprofiles of oxygen and nitrate in model sediment systems. Appl. Environ. Microbiol. **60:** 2094–2100.

JUNK, G., AND H. J. SVEC. 1958. The absolute abundance of the nitrogen isotopes in the atmosphere and compressed gas from various sources. Geochim. Cosmochim. Acta **14:** 234–243.

KEMP, M. J., AND W. K. DODDS. 2002*a*. Comparisons of nitrification and denitrification in prairie and agriculturally influenced streams. Ecol. Appl. **12:** 998–1009.

———, AND ———. 2002*b*. The influence of ammonium, nitrate, and dissolved oxygen concentrations on uptake, nitrification, and denitrification rates associated with prairie stream substrata. Limnol. Oceanogr. **47:** 1380–1393.

KENDALL, C., AND E. GRIM. 1990. Combustion tube method for measurement of nitrogen isotope ratios using calcium oxide for total removal of carbon dioxide and water. Anal. Chem. **62:** 526–529.

KNOX, M., P. D. QUAY, AND D. WILBUR. 1992. Kinetic isotopic fractionation during air–water gas transfer of O_2, N_2, CH_4, and H_2. J. Geophys. Res. **97:** 20335–20343.

LAURSEN, A. E., AND S. P. SEITZINGER. 2002. Measurement of denitrification in rivers: An integrated, whole reach approach. Hydrobiologia **485:** 67–81.

MCCUTCHAN, J. H., J. F. I. SAUNDERS, A. L. PRIBYL, AND W. M. J. LEWIS. 2003. Open-channel estimation of denitrification. Limnol. Oceanogr: Meth. **1:** 74–81.

MONTOYA, J. P. 1994. Nitrogen isotope fractionation in the modern ocean: Implications for the sedimentary record. *In* R. Zahn and others [eds.], Carbon cycling in the glacial ocean: Constraints on the ocean's role in global change. NATO ASI Series, Springer **117:** 259–279.

MULHOLLAND, P. J., AND OTHERS. 2002. Can uptake length in streams be determined by nutrient addition experiments? Results from an inter-biome comparison study. J. N. Am. Benthol. Soc. **21:** 544–560.

———, H. M. VALETT, J. R. WEBSTER, S. A. THOMAS, L. W. COOPER, S. K. HAMILTON, AND B. J. PETERSON. 2004. Stream denitrification and total nitrate uptake rates measured using a field ^{15}N tracer addition approach. Limnol. Oceanogr. **49:** 809–820.

NEWBOLD, J. D., J. W. ELWOOD, R. V. O'NEILL, AND W. VAN WINKLE. 1981. Measuring nutrient spiraling in streams. Can. J. Fish. Aquat. Sci. **38:** 860–863.

NIELSEN, L. P. 1992. Denitrification in sediment determined from nitrogen isotope pairing. FEMS Microbiol. Ecol. **86:** 357–362.

NIXON, S. W., AND OTHERS. 1996. The fate of nitrogen and phosphorus at the land-sea margin of the North Atlantic Ocean. Biogeochemistry **35:** 141–180.

PARR, R. N., AND S. A. CLEMENTS. 1991. Intercomparison of enriched stable isotope reference materials for medical and biological studies. International Atomic Energy Agency, NAHRES-5.

PETERSON, B. J., AND OTHERS. 2001. Control of nitrogen export from watersheds by headwater streams. Science **292:** 86–90.

PRESTON, S. D., AND J. W. BRAKEBILL. 1999. Application of spatially referenced regression modeling for the evaluation of total nitrogen loading in the Chesapeake Bay Watershed. U.S. Geological Survey Water-Resources Investigations Report 99-4054.

RABALAIS, N. N., R. E. TURNER, AND W. J. J. WISEMAN. 2001. Hypoxia in the Gulf of Mexico. J. Environ. Qual. **30:** 320–329.

RISGAARD-PETERSEN, N., S. RYSGAARD, L. P. NIELSEN, AND N. P. REVSBECH. 1994. Diurnal variation of denitrification and nitrification in sediments colonized by benthic microphytes. Limnol. Oceanogr. **39:** 573–579.

RUNKEL, R. L. 1998. One-dimensional transport with inflow and storage (OTIS): A solute transport model for streams and rivers. U.S. Geological Survey Water Resources Investigation Report 98-4018.

SEITZINGER, S. P. 1988. Denitrification in freshwater and coastal marine ecosystems: Ecological and geochemical significance. Limnol. Oceanogr. **33:** 702–724.

———, AND OTHERS. 2002. Nitrogen retention in rivers: Model development and application to watersheds in the eastern U.S. Biogeochemistry **57/58:** 199–237.

SIGMAN, D. M., K. L. CASCIOTTI, M. ANDREANI, C. BARFORD, M. GALANTER, AND J. K. BÖHLKE. 2001. A bacterial method for the nitrogen isotopic analysis of nitrate in seawater and freshwater. Anal. Chem. **73:** 4145–4153.

STREAM SOLUTE WORKSHOP. 1990. Concepts and methods for assessing solute dynamics in stream ecosystems. J. N. Am. Benthol. Soc. **9:** 95–119.

TOBIAS, C. R., M. CIERI, B. J. PETERSON, L. A. DEEGAN, J. VALLINO, AND J. HUGHES. 2003. Processing watershed-derived nitrogen in a well-flushed New England estuary. Limnol. Oceanogr. **48:** 1766–1778.

VALETT, H. M., J. A. MORRICE, C. N. DAHM, AND M. E. CAMPANA. 1996. Parent lithology, surface-groundwater exchange, and nitrate retention in headwater streams. Limnol. Oceanogr. **41:** 333–345.

WANNINKHOF, R., J. R. LEDWELL, AND W. S. BROECKER. 1985. Gas exchange-wind speed relation measured with sulfur hexafluoride on a lake. Science **227:** 1224–1226.

WEISS, R. F. 1970. The solubility of nitrogen, oxygen, and argon in water and seawater. Deep-Sea Res. **17:** 721–735.

Received: 2 July 2003
Amended: 9 December 2003
Accepted: 15 December 2003